ADVANCED MATERIALS
www.advmat.de

Ionic Gels for Low-Grade Heat Energy Harvesting and Thermal Sensing

Meng Xiao, Jianping Meng, Hulin Zhang, Zhiyi Wu, and Zhou Li**

Harvesting the low-grade heat energy from the environment and the human body remains an underutilized energy. Ionic thermoelectric (i-TE) gels have garnered significant attention in the fields of energy harvesting and sensing due to their exceptional stretchability, adaptability, ease of large-scale fabrication, and excellent thermoelectric performance. This review aims to provide a comprehensive overview of the recent progress of i-TE gels in application of temperature sensing and low-grade heat energy harvesting. The narration begins with the introduction of the synthetic and natural polymer for i-TE gels. Then, various methods are discussed to enhance the mechanical performance (stretchability, self-healing, and mechanical durability) to satisfy the flexible device based on i-TE gels. Noticeably, this work emphatically summarizes the improvement methods of thermopower for i-TE gels, including the preparation of n-type i-TE gels and the bidirectional modulation of their thermopower. Finally, this work explores the diverse applications of i-TE gels, including low-grade heat harvesting, sensing, human-machine interfaces, and biomedical applications.

1. Introduction

The pursuit of a sustainable and efficient power supply method for sensors has emerged as a focal point of research during the advancement of modern science and technology. The concept of harvesting energy from the environment to power sensors, thereby mitigating the need for frequent battery replacements, represents a promising avenue of investigation. Low-grade heat generated from the incomplete combustion of fossil fuels, the human body, and solar radiation remains an underutilized energy resource.[1] Thermoelectric materials have garnered increasing attention due to their capacity to directly convert heat into electricity. Conventional thermoelectric materials, such as commercial bismuth telluride (Bi_2Te_3), fail to meet the operational voltage requirements for sensors, which range from 1 to 5 V, even when a substantial number of arrays are integrated.[2]

Ionic thermoelectric (i-TE) materials have gained significant attention in comparison to traditional thermoelectric materials that utilize electrons as charge carriers, primarily due to their superior thermopower and high output voltage. The generation of high output voltage is attributed to ion diffusion and redox reactions occurring at the electrodes, which can match the working voltage of sensors. As an important member of ion thermoelectric materials, i-TE gels employ ions as carriers to convert heat into electricity, which is a sustainable and environmentally friendly technology. In contrast to liquid thermocells, i-TE gels present several advantages, including flexibility, nonleakage properties, and enhanced thermopower. These attributes enable efficient performance at ambient temperatures, making them suitable power supply for self-powered sensors and wearable technologies. Nevertheless, current i-TE gels underperform in critical parameters such as thermopower and output power density, which poses challenges in fulfilling the requirements for practical applications.

The development milestones of thermionic capacitors and thermocells are illustrated (**Figure 1**).[3–11] In 2016, Zhao et al. defined thermionic capacitors as devices capable of harvesting electricity from the electric double layer present at the electrode.[12] These thermionic capacitors can effectively capture energy from intermittent heat sources, such as solar radiation. In the same year, Yang et al. developed a wearable thermocell based on thermogalvanic gel electrolytes to harvest energy from body heat.[13] By modulating the interactions between ions and the polymer matrix, the thermopower of i-TE gels can be adjusted from negative to positive values.[5] Through the investigation of various electrolytes and the integration of thermocells into thermoelectric modules, the output voltage of these thermocells has been

M. Xiao, J. Meng, Z. Wu
Beijing Institute of Nanoenergy and Nanosystems
Chinese Academy of Sciences
Beijing 101400, China
E-mail: wuzhiyi@binn.cas.cn
H. Zhang
College of Integrated Circuits
Taiyuan University of Technology
Taiyuan 030024, China
Z. Li
Tsinghua Changgung Hospital
School of Clinical Medicine
Tsinghua University
Beijing 100084, China
E-mail: li_zhou@tsinghua.edu.cn
Z. Li
School of Biomedical Engineering
Tsinghua University
Beijing 100084, China

The ORCID identification number(s) for the author(s) of this article can be found under https://doi.org/10.1002/adma.202506436

DOI: 10.1002/adma.202506436

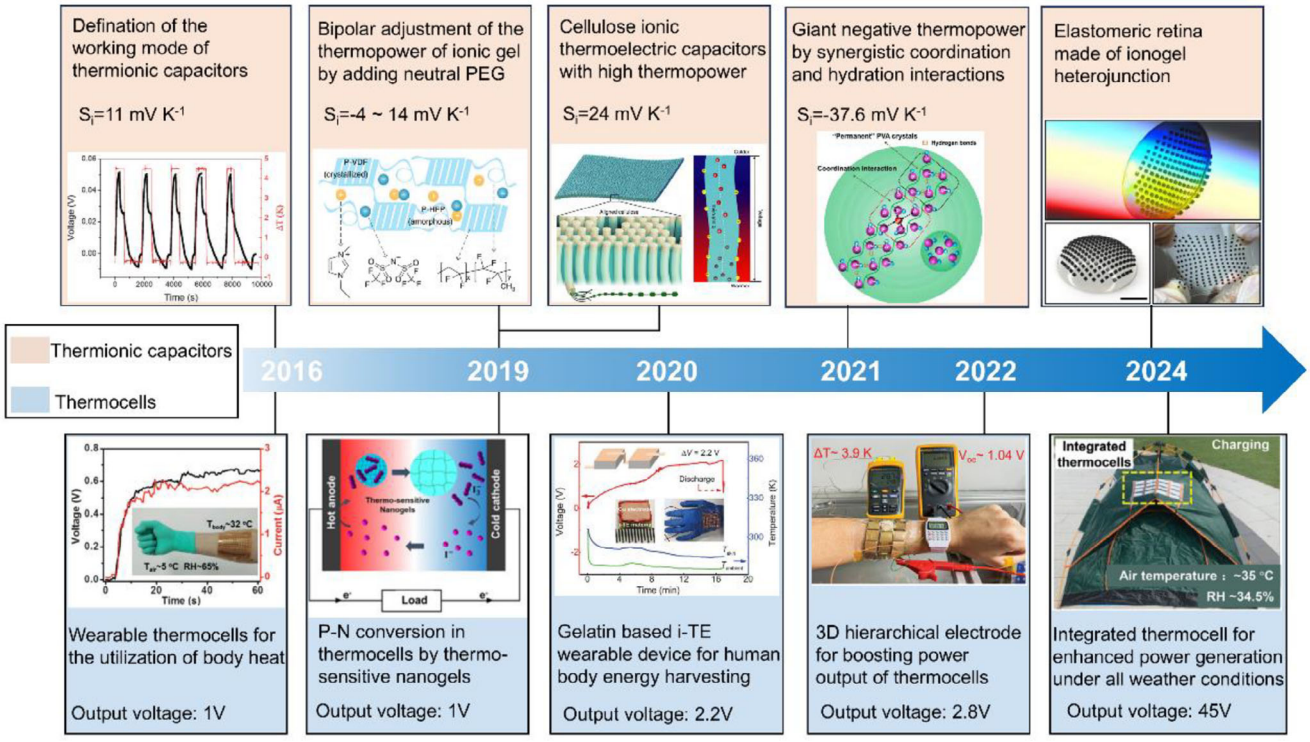

Figure 1. Milestones of ionic gels in the development of thermionic capacitors and thermocells. Reproduced with permission.[12] Copyright 2016, Royal Society of Chemistry. Reproduced with permission.[13] Copyright 2016, Wiley-VCH. Reproduced under the terms of the CC-BY 4.0 license.[4] Copyright 2019, The Authors, Springer Nature. Reproduced with permission.[3] Copyright 2019, Elsevier. Reproduced with permission.[5] Copyright 2019, The Authors, Springer Nature. Reproduced with permission.[6] Copyright 2020, The Authors, The American Association for the Advancement of Science (AAAS). Reproduced with permission.[8] Copyright 2021, The Authors, The American Association for the Advancement of Science (AAAS). Reproduced with permission.[9] Copyright 2022, Wiley-VCH. Reproduced under the terms of the CC-BY 4.0 license.[10] Copyright 2024, The Authors, Springer Nature. Reproduced with permission.[11] Copyright 2024, Wiley-VCH.

continuously enhanced. The applications of i-TE gels encompass a wide range, including energy harvesting, thermal sensing, human-machine interfaces, and biomedical applications.[10]

This review aims to design guideline of i-TE gels characterized by superior mechanical properties and enhanced thermoelectric performance, including high thermopower, output power density (**Figure 2**). The narration will commence with an overview of the development of i-TE gels. Subsequently, we will provide a brief introduction to the operational modes of i-TE gels, encompassing thermionic capacitors and thermocells. In terms of material composition, this review will concentrate on i-TE gels synthesized from both synthetic and natural polymers. To enhance the longevity of i-TE gels under challenging operational conditions, we will focus on their mechanical durability, stretchability, and self-healing properties. Furthermore, methods to modulate thermopower, including the development of p-type, n-type, and p-n conversion of i-TE gels, ion doping, structural engineering, ion-electron coupling, as well as the design of electrodes and electrolytes, are presented. Finally, we will explore the applications of i-TE gels in various fields, including low-grade heat harvesting, thermal sensing, human-machine interfaces, and biomedical applications. The review will also address the challenges and future perspectives associated with i-TE gels, aiming to further elucidate their potential.

2. The Energy Conversion Mechanism and Working Mode of i-TE Gels

2.1. The Energy Conversion Mechanism of i-TE Gels

Early investigations into i-TE materials primarily focused on ionic solutions or molten salts.[25] However, compared to i-TE solutions, quasi-solid i-TE gels composed of organic components exhibit significantly high thermopower, ranging from several to tens of millivolts per Kelvin (mV K^{-1}). Additionally, i-TE gels present several advantages, including flexibility, and the potential for large-scale fabrication, rendering them suitable for applications in flexible electronic devices.[26–28]

When a temperature difference (ΔT) is applied across a gel electrolyte, charge carriers, like cations and anions, diffuse from the cold side to the hot side until the open-circuit voltage (ΔV_{max}) counterbalances further ion diffusion. The thermopower, or the ionic Seebeck coefficient, describes the performance of heat-to-electricity conversion in i-TE materials.[29,30] Generally, the thermopower is defined as:

$$S_i = -\frac{V(T_H) - V(T_C)}{T_H - T_C} \quad (1)$$

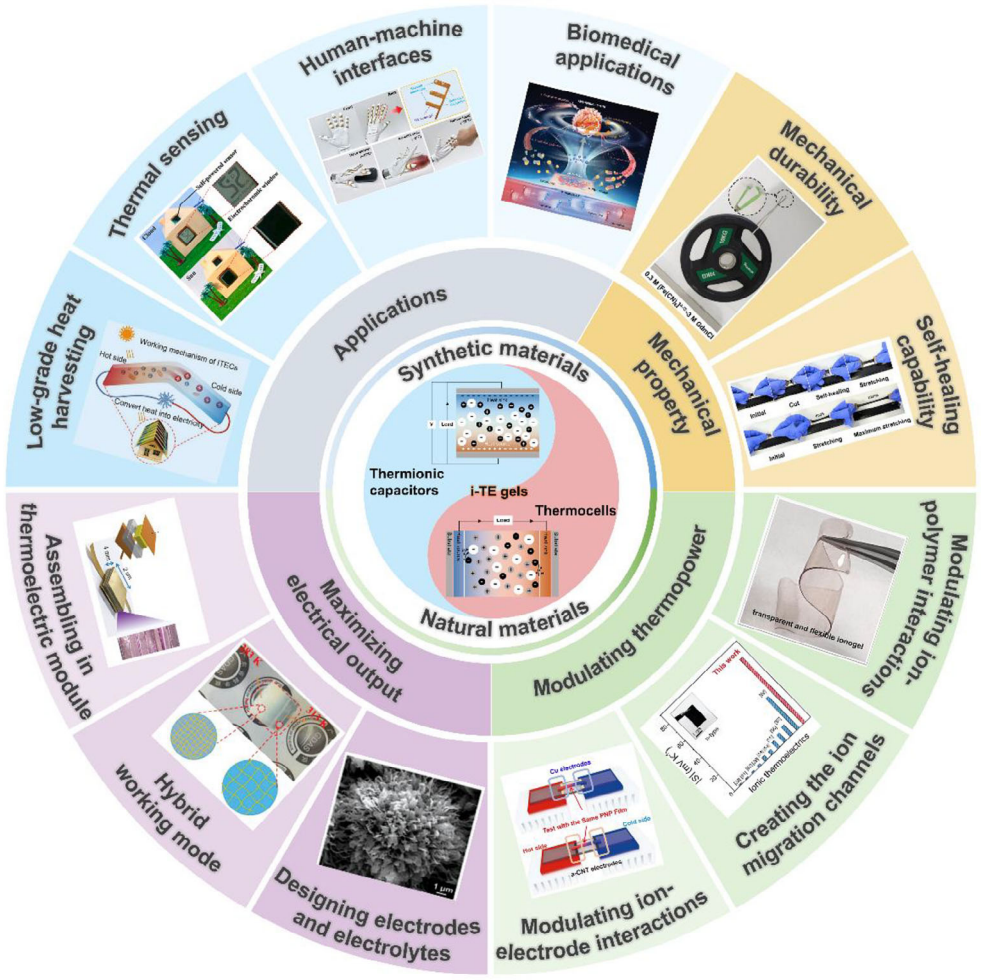

Figure 2. The working mode of i-TE gels can be classified into either thermionic capacitors or thermocells. Reproduced with permission.[14] Copyright 2022, The Authors, Springer Nature. Reproduced with permission.[15] Copyright 2024, Elsevier. Reproduced under the terms of the CC-BY 4.0 license.[16] Copyright 2023, Wiley-VCH. Reproduced with permission.[17] Copyright 2025, Wiley-VCH. Reproduced with permission.[18] Copyright 2023, Wiley-VCH. Reproduced under the terms of the CC-BY 4.0 license.[19] Copyright 2023, The Authors, Springer Nature. Reproduced with permission.[20] Copyright 2023, Elsevier. Reproduced with permission.[21] Copyright 2024, Wiley-VCH. Reproduced under the terms of the CC-BY 4.0 license.[22] Copyright 2023, The Authors, Springer Nature. Reproduced with permission.[9] Copyright 2022, Wiley-VCH. Reproduced with permission.[23] Copyright 2023, Wiley-VCH. Reproduced with permission.[24] Copyright 2024, Wiley-VCH.

where $V(T_H)$ and $V(T_C)$ represent the voltages of the hot and cold electrodes at temperatures T_H and T_C, respectively. The sign of thermopower defines the type of dominant ion carriers in i-TE gels, which is p-type ($S_i > 0$) for cations and n-type ($S_i < 0$) for anions. The sign of thermopower is related to the average transport entropy per carrier charge (on the order of mV/K for i-TE gels).

The high thermopower of i-TE gels originate from different heat-to-electricity conversion mechanism, including the thermodiffusion effect, thermogalvanic effect, thermoextraction effect and the synergistic effect (**Figure 3**a–c).[31] The thermodiffusion effect originate from the Soret effect. Under a ΔT, the thermodiffused ions accumulate at the electrode, generating an open-circuit penitential that can drive current through the external circuit. The heat energy can be converted into electricity by working in a supercapacitor mode. The thermogalvanic effect requires temperature difference specific redox ions and electron cycling. Under ΔT, redox ion pairs diffused form the hot side to cold side, where redox reactions occur at the electrode, generating an electron current in the external circuit. The thermogalvanic effect leads to an i-TE generator which can output consistent current under a temperature difference. The thermoextraction effect can be concluded into ion-electrode interactions. Typically, the cations inserted in positive electrodes can be extracted and transported to negative electrode under temperature gradient. Generally, i-TE gels based on single thermodiffusion effect has high thermopower but low power density limited by low ionic conductivity. In contrast, i-TE gels that utilize the thermogalvanic effect achieve high power density while exhibiting low thermopower. By synergistically utilizing both thermodiffusion and thermogalvanic effect, the thermopower and output power density can be improved at the same time.

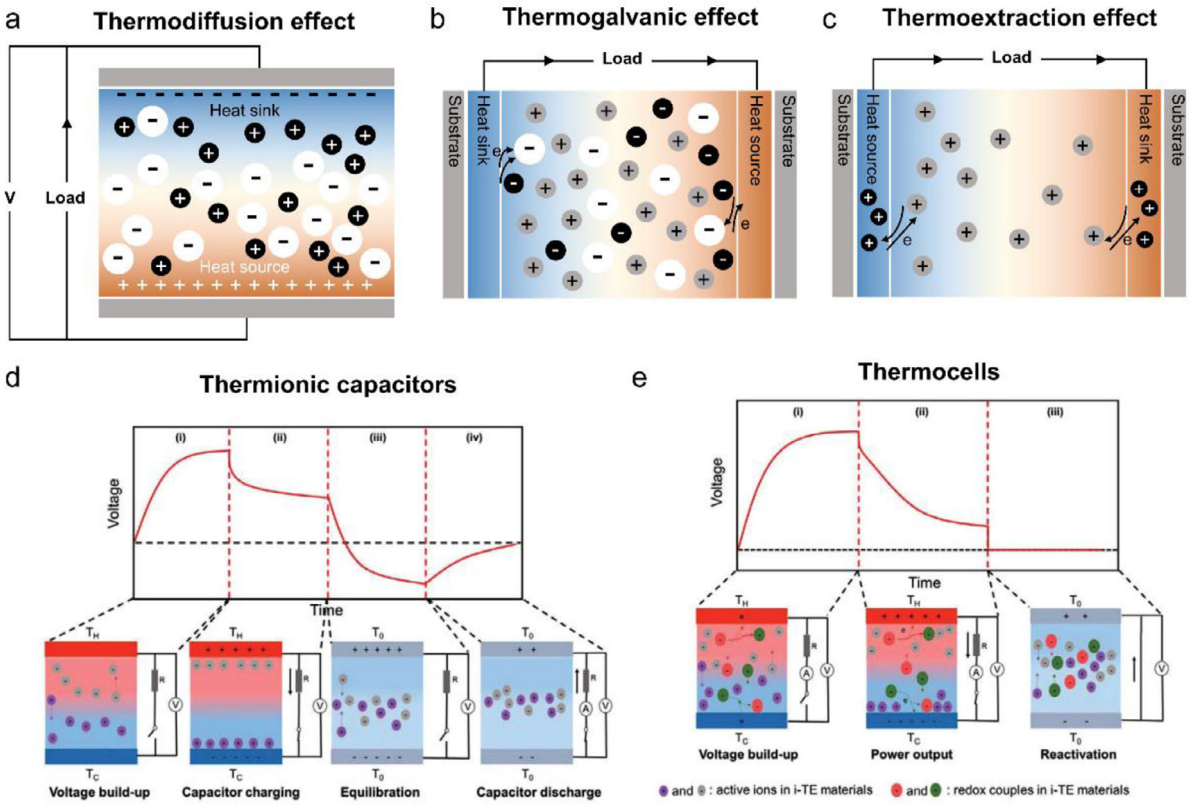

Figure 3. Schematic illustration of energy conversion mechanism of i-TE gels for a) thermodiffusion effect, b) thermogalvanic effect, c) thermoextraction effect. Schematic illustration of the working mode of d) thermoionic capacitors and e) thermocells. Reproduced with permission.[9] Copyright 2022, Wiley-VCH.

2.2. The Working Mode of i-TE Gels

Depending on their operational principles, i-TE gels can function as either thermionic capacitors or thermocells (Figure 3d,e).[32] The thermodiffused ions accumulate near the electrode and form an electrical double layer. Thereby, an open-circuit potential was generated that can cause a current flow through the external load. In 2016, X. Crispin proposed the working mechanism of thermionic capacitor, which can be divided into four stages: (i) voltage built-up, (ii) capacitor charging, (iii) equilibration, (iv) capacitor discharge.[12] In the first step, an open-circuit voltage was established under a stable ΔT. Then, an external load was connected to the electrode, with an electric current pass through the external load while maintaining a ΔT. In the third step, both the ΔT and external load was removed from circuit. It is worth mentioned that the ions in the i-TE gels diffuse back while the attracted charges at the electrodes still remain. Driven by the stored charges, the open-circuit voltage decreases to zero and continue decline to a negative value. Finally, the negative charges pass through the external load and form an opposite direction current compared with step ii. The thermionic capacitor can convert heat into electricity by harvesting intermittent heat source. The output energy can be calculated by the following equation:

$$E = \frac{1}{2} C \left(\Delta T S_i\right)^2 \tag{2}$$

where C, ΔT, S_i represent the specific capacitance, thermopower, and temperature difference for this device, respectively.

In thermocells, redox ion pairs diffuse from the hot side to the cold side, where redox reactions occur at the electrodes, generating a consistent current in the external circuit. Typically, the heat-to-electricity conversion of thermocells contain three steps, without energy storage process. The first step is the same as in thermionic capacitors, an open-circuit voltage was generated under ΔT. Next, by connecting with an external load, the voltage and current gradually decline under ΔT. In the third step, the thermocell is connected in a short-circuit condition, corresponding to a reactivation process. The output energy in the second step can be defined as:

$$E = \int_0^{t_{ii}} V(t)\, I(t)\, dt \tag{3}$$

where t_{ii}, V(t), I(t) are the output energy time, V(t) and I(t) are the corresponding voltage at specific time, respectively.

The maximum instantaneous power density (P_{max}) refers to the ratio of maximum power the device can output to the external load resistance under a certain temperature difference to the electrode area. The normalized maximum instantaneous power density ($P_{max}/\Delta T^2$) is the ratio of P_{max} to the square of the temperature difference, which represents a key parameter for evaluating the output performance of i-TE gels. The normalized maximum

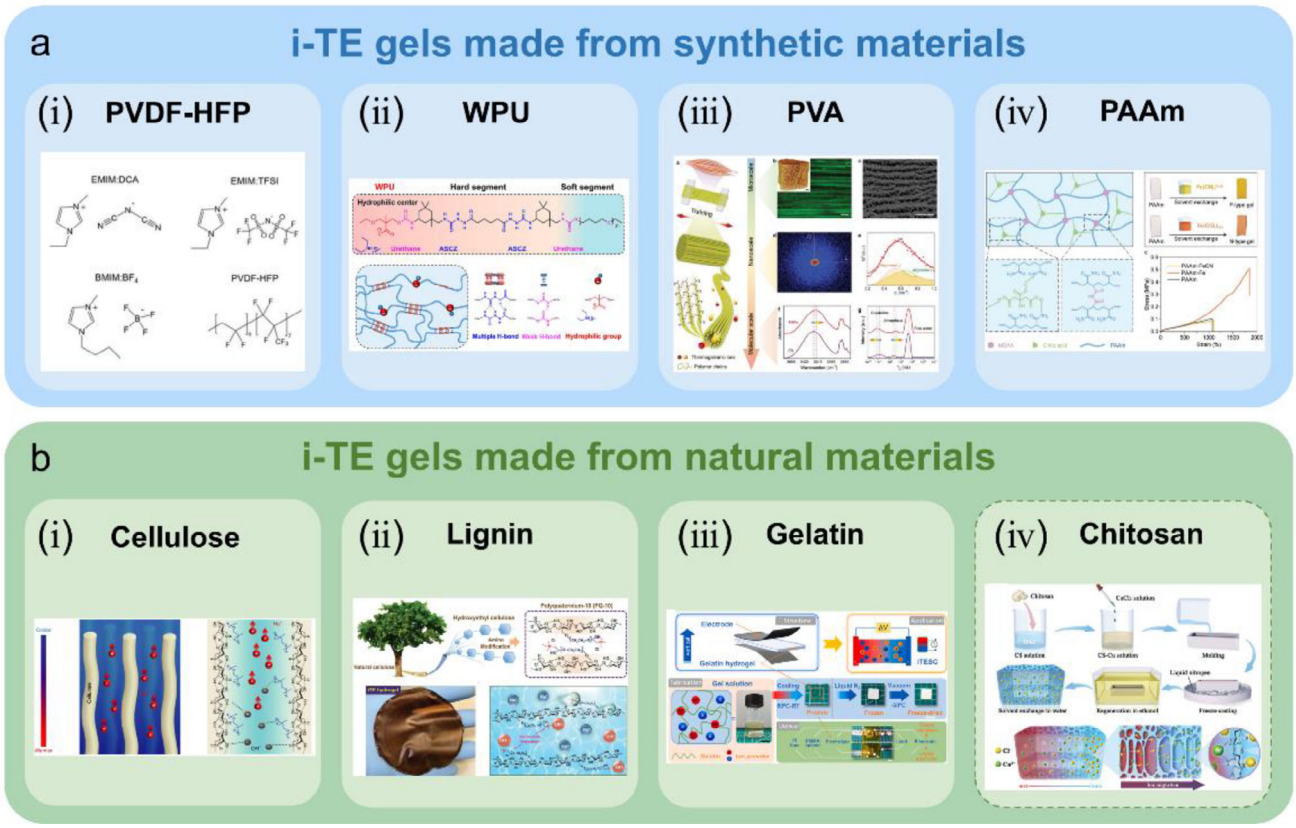

Figure 4. i-TE gels made from synthetic and natural materials. a). i-TE gels made from synthetic materials, like i) PVDF-HFP,[35–38] Reproduced with permission.[34–38] Copyright 2019, Wiley-VCH. ii) WPU,[39–41] Reproduced with permission.[14,39–41] Copyright 2022, The Authors, Springer Nature. iii) PVA,[67,68] Reproduced with permission.[45,67,68] Copyright 2019, Wiley-VCH. (iv) PAAm, Reproduced with permission.[43] Copyright 2022, Wiley-VCH. b) i-TE gels made from natural materials, like i) Cellulose,[16,46,57–60] Reproduced with permission.[4,16,46,57–60] Copyright 2019, The Authors, Springer Nature. ii) Lignin,[61] Reproduced with permission.[16,61] Copyright 2023, Wiley-VCH. iii) Gelatin,[6,7,20,51–53] Reproduced with permission.[6,7,20,51–54] Copyright 2024, Elsevier. iv) Chitosan.[56] Reproduced with permission.[55,56] Copyright 2024, Wiley-VCH.

power density is calculated when the external load resistance is equal to the internal resistance of the cell, as expressed below:

$$P_{max}/\Delta T^2 = V_{oc} I_{sc}/4\Delta T^2 \quad (4)$$

where V_{oc} and I_{sc} represent the open-circuit voltage and short-circuit current, respectively.

3. i-TE Gels Materials

3.1. i-TE Gels based on Synthetic Materials

I-TE gels can be fabricated by either synthetic or natural materials. The common components of i-TE gels contain polymer matrix, thermodiffused ions and redox ion pairs (**Table 1**).[33] The polymer matrix may consist of poly(vinylidene fluoride-*co*-hexafluoropropylene) (PVDF-HFP),[34–38] waterborne polyurethane (WPU),[14,39–41] polyethylene oxide (PEO),[12,42,43] polyvinyl alcohol (PVA),[18,44,45] and crosslinked polymer networks.[43,46–49] Cheng et al. developed a quasi-solid-state ionogel composed of PVDF-HFP and the ionic liquid (1-ethyl-3-methylimidazolium dicyanamide, EMIM:DCA), achieving a remarkable thermopower of up to 26.1 mV K^{-1} (**Figure 4ai**).[34] This high thermopower is attributed to the interaction between ions and dipole segments of PVDF-HFP. To synergistically enhance both ionic conductivity and thermopower, Li et al. incorporated ethanol and sodium bis(trifluoromethylsulfonyl)imide (NaTFSI) into the polymer network, fabricating the PVDF-HFP/EMIM:DCA ionogels.[38] Subsequently, a wearable wristband with five legs was developed based on the ionogel fiber, which exhibited improved thermoelectric performance, mechanical properties, and wearing comfort, generating a high thermovoltage of 119.1 mV at room temperature (ΔT = 2.7 K).

Polyurethane can serve as a polymer matrix to enhance the mechanical properties of the ionogels. Fang et al. prepared stretchable and transparent ionogels by mixing elastomeric WPU with EMIM:DCA.[39] The ionogels containing 40 wt% EMIM:DCA exhibited a high thermopower of 34.5 mV K^{-1}, ionic conductivity of 8.4 mS cm^{-1} at a relative humidity of 90%. To further enhance the i-TE performance of the stretchable ionogels, Xiao et al. fabricated a nanocomposite ionogel by incorporating laponite nanosheets and ionic liquid into WPU (Figure 4aii).[14] The negatively charged laponite nanosheets and released Na^+ ions can increase the thermophoretic mobility difference between cations and anions and achieve thermopower. The nanocomposite ionogel demonstrates high i-TE performance (S_i = 44.1 mV K^{-1},

Table 1. Summary and comparisons of i-TE performance of gels made from synthetic and natural materials.

Materials	S_i [mV K^{-1}]	σ_i [mS cm^{-1}]	λ [W m^{-1} K^{-1}]	PF_i [mW m^{-1} K^{-2}]	Humidity [%]	Ref.
PVDF-HFP/EMIM:DCA	26.1	6.7	0.18	0.46	85	[34]
PVDF-HFP/EMIM:DCA/NaDCA	43.8	19.4	0.18	3.72	85	[35]
WPU/EMIM:DCA	34.5	8.4	0.23	1.00	90	[39]
WPU/Laponite/EMIM:DCA	44.1	14.1	2.74	2.74	90	[14]
PEO/NaOH	10.0	0.1		0.01		[12]
PEO/LiTFSI/EMIM:BF_4	15.0	1.9		0.04		[42]
PVA/HCl	38.2	18.9	0.46	2.75		[67]
PVA/CsI	52.9	51.5	0.54	14.41		[68]
PANI/PAAMPSA/PA	8.1	237	0.45	1.55		[69]
PPP/SiO_2/NPs	17.9	187	0.48	5.99		[70]
Cellouse/NaOH	24.0	20.0	0.48	1.15		[4]
CNF/ChCl:EG	18.0	7.2	0.19	0.23	60	[60]
BC/EMIM:DCA	18.0	28.8	0.21	0.93		[62]
BC/EMIM:DCA/NaDCA	45.0	21.2		4.3	85	[59]
Gelatin/EMIM:Ac/acetate salts	37.3	12.3	0.24	1.71		[20]
PVA/Chitosan/$CuCl_2$	28.4	40.5	0.49	3.27		[55]
Lignin/KOH	30.4	5.9	0.36	0.54		[61]

σ_i = 14.1 mS cm^{-1}) at a relative humidity of 90%. Given the toxic properties of ionic liquids, Zhao et al. developed a eutectogel by incorporating WPU and an eco-friendly deep eutectic solvent (ChCl:EG).[41] These eutectogels exhibit a high mechanical stretchability of 216% while maintaining high i-TE performance (S_i = 19.5 mV K^{-1}, σ_i = 8.4 mS cm^{-1}) at the same relative humidity.

Generally, thermal sensors based on brittle semiconductor thermoelectric materials struggle to produce a stable current when subjected to stretching. In contrast, i-TE gels with intrinsic stretchability are capable of converting heat into electricity even after undergoing thousands of stretching cycles. Additionally, Lei et al. presented an anti-fatigue and highly conductive thermocell characterized by hierarchical fibrils and aligned nanochannels, achieved through bionic mechanical training (Figure 4aiii).[45] The long-term mechanical properties of the thermocell are significantly enhanced without compromising its thermoelectric power density.

Hydrogel-based electrolytes are susceptible to dehydration in ambient conditions. Part et al. developed fully stretchable ionic thermoelectric supercapacitors (ITESCs) with exceptional air stability (>60 days) (Figure 4aiv).[47] The ITESCs consists of a stretchable i-TE elastomer electrolyte and stretchable gold nanowire electrodes. The i-TE gel exhibits a high thermopower (38.9 mV K^{-1}) and a high ionic conductivity (3.76 × 10^{-1} mS cm^{-1}) at 90% relative humidity, along with reliable mechanical stability, as demonstrated by its ability to endure 500 cycles of 50% strain.

3.2. i-TE Gels based on Natural Materials

Although synthetic polymers are commonly used in i-TE materials, environmental concerns have arisen due to the challenges associated with recycling these materials.[50] Biopolymers and their derivatives, known for their abundance, environmental friendliness, and biocompatibility, have garnered significant interest in the field of i-TE materials. Biopolymers such as gelatin,[6,7,20,51–54] chitosan,[55,56] cellulose,[4,16,46,57–60] lignin,[61] and bacterial cellulose[54,62–66] serve as ideal matrices for i-TE materials, particularly for large-scale production and on-skin applications.

Li et al. utilized the hierarchical alignment structure of cellulose to fabricate an ionic conductor by infiltrating an electrolyte into a nanofluidic cellulose membrane (Figure 4bi).[4] The negatively charged groups along the aligned cellulose molecular chains facilitate the movement of Na^+ ions while hindering the transport of OH^- ions, resulting in a substantial thermopower of 24 mV K^{-1}. This work inspired us to leverage the structural characteristics of natural materials to create pathways for directional ion movement and to fabricate ionic conductors with high thermopower for low-grade heat harvesting. In contrast to the mechanism described by Li et al., Han et al. demonstrated a high-performance i-TE gel composed of polyquaternium-10 (PQ-10), a cellulose derivative, as the polymer matrix and sodium hydroxide (NaOH) as the ion source (Figure 4bii).[16] The cationic quaternary amino groups on the PQ-10 polymer chains attract hydroxide ion (OH^-) through electrostatic interactions, while Na^+ can move freely under a temperature gradient, resulting in a high

thermopower of 24.2 mV K^{-1}. A smart glove is developed using PQ-10/NaOH thermal sensor arrays, demonstrating the potential application of i-TE hydrogels in artificial systems. Smart gloves based on i-TE hydrogels hold significant promise for applications in mechanical intelligence and human-machine interfaces.

Ye et al. presented an ultrastretchable and tough ionogel based on water-induced competitive hydration interactions.[46] By regulating the intermolecular interactions between cellulose nanofibers (CNF), water, and ionic liquid (IL), the ionogels demonstrate significantly enhanced mechanical performance and ionic conduction. Additionally, the strong interactions between the IL and water improve the environmental stability of the ionogels by suppressing water freezing and evaporation. Gelatin is an ideal biopolymer for fabricating i-TE hydrogels. Han et al. prepared a quasi-solid i-TE hydrogel using gelatin as the matrix and harnessing the synergistic effect of thermodiffusion and thermogalvanic.[6,7] A flexible i-TE wearable device with 25 p-type elements exhibits a high voltage up to 2.2 V, which is two to three times higher than that of previously reported i-TE devices. The fabricated i-TE cells can operate in continuous mode, generating a maximum energy density of 12.8 J m^{-2}. Recent studies have highlighted the synergy between hydrogel electrolytes and electrodes in enhancing the thermopower and energy density of i-TE devices. Xu et al. demonstrates the influence of electrodes on the tunable i-TE performance of gelatin-based ITESCs (Figure 4biii).[54] After replacing the conventional copper foil with carbon-based paper electrodes, the thermopower of Gelatin-CsCl transitioned from p-type to n-type due to the restricted cation mobility.

Inspired by plant stems, Sun et al. present a chitosan/$CuCl_2$ hydrogel (ChCu) with a notable negative thermoelectric coefficient (Figure 4biv).[55] Using freeze-casting technology and Cu^{2+} complexation with chitosan, ChCu has a layered porous structure. In a temperature gradient, most Cu^{2+} is immobilized in the chitosan matrix, while unbound Cu^{2+} migrates thermally, intercepted by the layered architecture. In contrast, Cl^- migrates freely toward the colder end and accumulates, facilitating selective migration and distribution of ions and counterions. Consequently, ChCu exhibits a thermoelectric coefficient of −23.8 mV K^{-1} and generates a voltage of 4.0 mV under a minimal temperature difference (ΔT = 0.3 K). Hu et al. introduced a novel approach to enhance thermopower and output power by leveraging the synergy of the thermodiffusion effect and thermogalvanic effect in an ionic gel electrolyte containing a single redox component (CG-MA gels).[56] The biguanide groups grafted onto the gel network accelerate the selective separation of positive and negative ions, resulting in an enhanced thermodiffusion effect. The incorporation of melamine into the gel networks facilitates the selective complexation and desorption of Fe^{3+} at the cold end, thereby enhancing the thermogalvanic effect. Consequently, the optimized CG-MA gels achieve a high thermopower of −7.2 mV K^{-1} and a maximum instantaneous power density of 4.5 W m^{-2}, along with a record-breaking output energy density of 17.9 kJ m^{-2}.

4. Mechanical Performance and Self-Healing Performance of i-TE Gels

By continuously converting waste heat from the environment into electricity, i-TE gels can serve as ideal power sources for flexible electronic devices. Excellent mechanical performances, such as stretchability, and mechanical durability will significantly expand their applications in the wearable technology field.[71] Additionally, self-healing performance is also an indispensable performance for application.

4.1. Designing the Network Structure of i-TE Gels

Although the thermoelectric performance of ionic gels can meet energy supply requirements, inadequate mechanical performance remains a challenge. This limitation restricts the sustainability and longevity of i-TE gels in practical applications. A critical challenge in the advancement of i-TE devices lies in the enhancement of mechanical properties without compromising i-TE performance, which is essential for prolonging service life and broadening operational scenarios. Researchers have investigated multiple approaches to optimize the network structures of ionic hydrogels to enhance their mechanical performance, including stretching-induced crystallization,[18,45] double-network structures,[49,72–74] and the enhancement of molecular entanglements.[44,75–77]

Inspired by muscle myogenic fibers, Liu et al. developed a quasi-solid stretchable thermocell based on polyvinyl alcohol (PVA) by utilizing stretching-induced crystallization and redox couple ion exchange (**Figure 5a**).[18] The mechanical performance of the i-TE gel are enhanced due to the formation of a hierarchical anisotropic network formed by freezing-casting-assisted stretching. Consequently, the i-TE gel demonstrated an enormous tensile strength of 19 MPa and a high thermopower of 6.5 mV K^{-1}. In contrast, i-TE gels that conform to the curved surface maintain stable temperature perception even when stretched. Zhao et al. developed an ultra-stretchable hydrogel thermocouple for temperature sensing during stretching.[78] This thermocouple demonstrates a high thermopower of 1.93 mV K^{-1} with a pair of p/n junction and exhibits stable sensing behavior under a tensile strain of 100%. Additionally, a virtual reality glove utilizing thermally driven artificial muscles is fabricated to provide kinesthetic haptic feedback.

Quasi-solid thermocells are vulnerable to breakage due to low fracture energy, which limits their use. Improving the mechanical properties of i-TE gels involves optimizing their network structure, but higher crosslinking density can impede ion thermodiffusion and reduce i-TE performance. Therefore, an optimal design must balance mechanical strength and i-TE performance. Lei et al. developed double network thermocells with remarkable toughness of 2270 J m^{-2}, notch insensitivity, and an enhanced normalized maximum power density of 0.61 mW m^{-2} K^{-2} (Figure 5b).[73] The initial charged network interacts with the redox ion couple, thereby augmenting the thermopower. Notably, the second network synergistically enhances the first network by reducing interfacial energy and increasing energy dissipation, which in turn improves the toughness of the thermocell. Achieving a balance between high toughness and good elasticity in thermocells remains a significant challenge. Lyu et al. developed a thermocell with a dense network structure by increasing the monomer concentration and decreasing the content of the cross-linking agent (Figure 5c).[77]

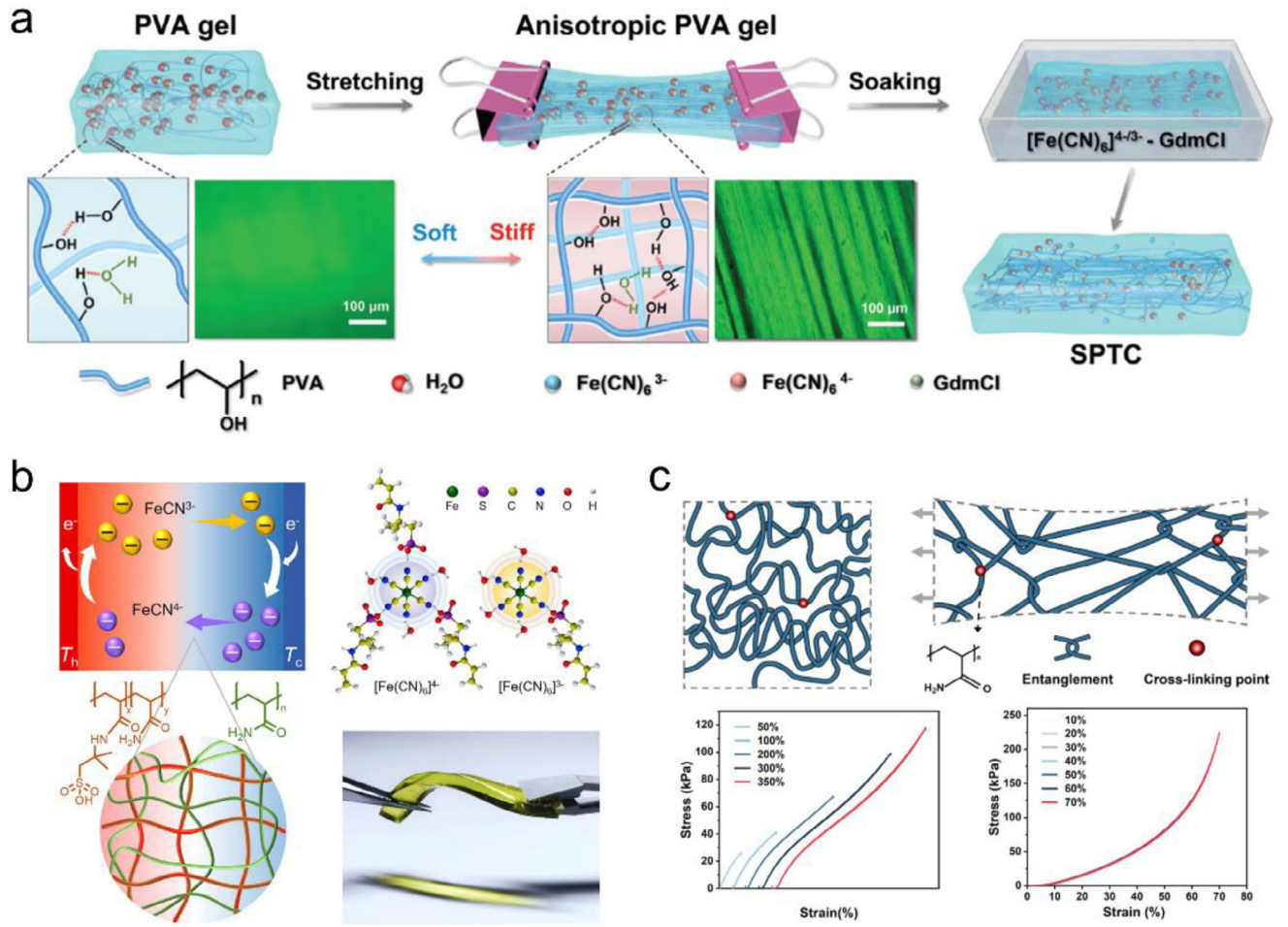

Figure 5. Improving the mechanical properties of i-TE gels through network structure design. a). A robust and durable thermogalvanic hydrogel with high thermoelectric performance is achieved through stretching-induced crystallization. Reproduced with permission.[18] Copyright 2023, Wiley-VCH. b). Double network thermocells demonstrate exceptional toughness and enhanced power density for continuous heat harvesting. Reproduced with permission.[73] Copyright 2021, Elsevier. c). A tough and elastic hydrogel thermocell showcases a dense network structure optimized for low-grade heat harvesting. Reproduced with permission.[77] Copyright 2024, Elsevier.

By enhancing molecular entanglements, these thermocells effectively mitigate the trade-off between elasticity and toughness.

4.2. Self-Healing Behavior of i-TE Gels

The self-healing properties of i-TE gels are poised to significantly influence the fields of robotics and prosthetics, as these materials can be worn for extended periods without the risk of damage. Moreover, their self-healing capability allows for recovery from minor injuries, thereby enhancing both their lifespan and cost-effectiveness.[37] The self-healing behavior of i-TE gels and their applications in devices will be discussed separately.

Kim et al. developed a self-healable polymer, PEDOT:PAAMPSA:PA, which exhibited remarkably high i-TE properties (**Figure 6a**).[19] The polymer demonstrates excellent durability of i-TE performance under cyclic self-healing (30 cycles) and stretching processes (50 cycles). The i-TE devices achieve a maximum power output and energy density of 4.59 $\mu W \cdot m^{-2}$ and 1.95 $mJ \cdot m^{-2}$, demonstrating its potential for self-powered wearable devices. Malik et al. demonstrated a self-healable organic-inorganic i-TE composite (OITC) by incorporating SiO_2 nanoparticles into a ternary polymer of PANI:PAAMPSA:PA (Figure 6b).[69,70] The incorporation of SiO_2 nanoparticles enhance the i-TE performance of the OITC by promoting the ion dissociation of functional groups within the polymer. The OITC exhibits improved i-TE performance (S_i = 17.9 mV K^{-1}) compared to the organic polymer (S_i = 15.0 mV K^{-1}) at 80% relative humidity.

In most cases, thermoelectric modules are fabricated on rigid substrates and electrodes, despite the self-healing capabilities of i-TE materials, which limit their mechanical stretchability and suitability for wearable applications. To address this challenge, Ho et al. developed a zwitterionic copolymer-based fully self-healable ionic thermoelectric generator (TEG) (Figure 6c).[79] The copolymer-based TEG exhibited rapid self-healing ability at room temperature due to the multiple ionic interactions of

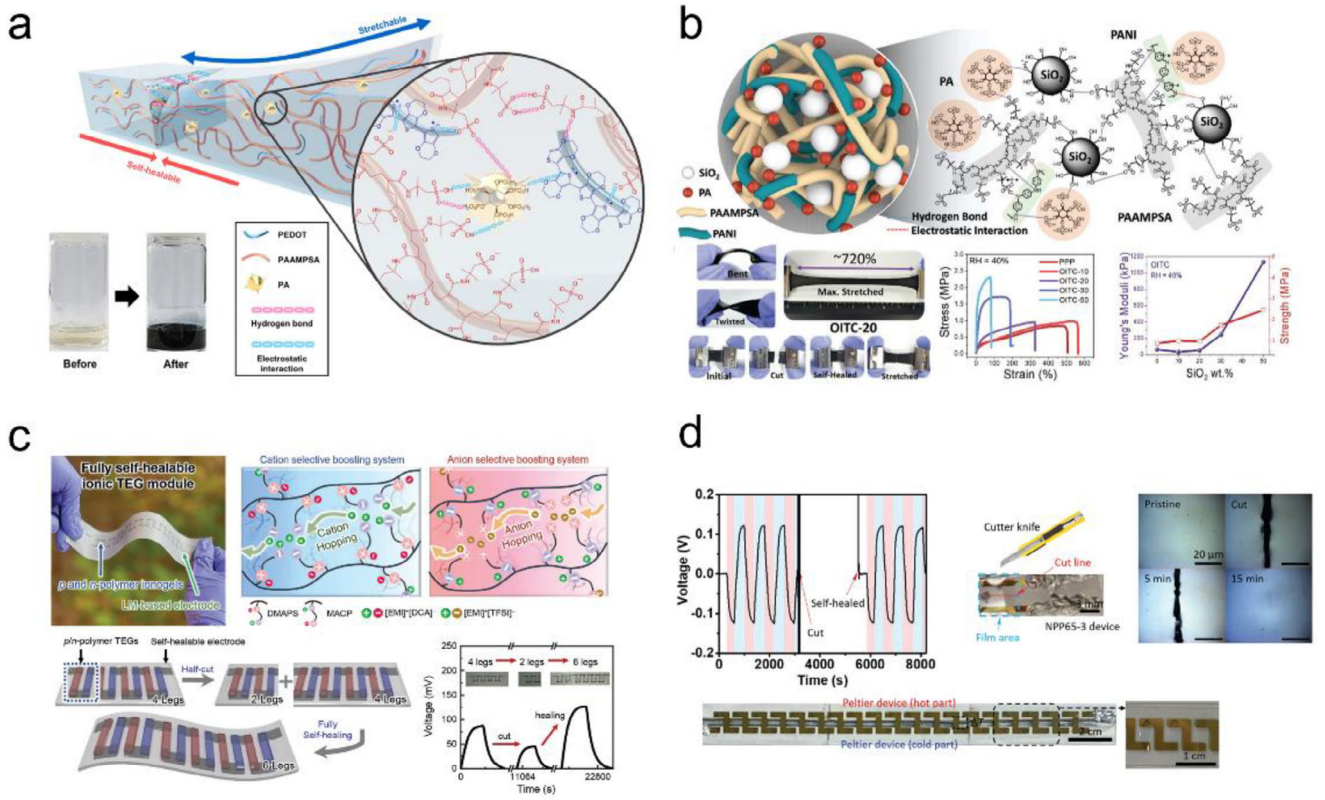

Figure 6. Self-healing behavior of i-TE gels. a) Stretchable and self-healable polymer, PEDOT:PAAMPSA:PA, exhibits remarkably high i-TE properties. Reproduced under the terms of the CC-BY 4.0 license.[19] Copyright 2023, The Authors, Springer Nature. b) Self-healable organic-inorganic hybrid thermoelectric materials demonstrate excellent i-TE performance. Reproduced with permission.[70] Copyright 2021, Wiley-VCH. c) A fully self-healable i-TE module is based on zwitterionic polymer gels. Reproduced with permission.[79] Copyright 2023, Wiley-VCH. d) A wearable and transparent thermoelectric hydrogel, which utilizes bisulfate transport, features a large negative thermopower. Reproduced with permission.[80] Copyright 2022, Royal Society of Chemistry.

zwitterionic groups present in the side chains. Additionally, a self-healing electrode composed of WPU, PVA, and liquid metal has been created for fully self-healable TEG. A fully healable TEG with ten legs is constructed using p-type and n-type ionogels. Through the cutting and healing process, the legs of the TEG module can be modified to different quantities, allowing the voltage to be adjusted to the desired level, thereby demonstrating modularity and replaceability.

Most ionogels fabricated with ionic liquids are toxic, posing environmental risks regarding disposal situation after use. Thermoelectrics with a non-hazardous and eco-friendly composition hold significant potential for large-scale low-grade energy conversion. Cho et al. developed a wearable and transparent thermoelectric hydrogel based on bisulfate transport (Figure 6d).[80] For the first time, biocompatible bisulfate is utilized as a thermally diffusive anion carrier in a thermoelectric device. The i-TE hydrogel achieves a negative thermopower of −25 mV K^{-1} and an ionic figure of merit of 7.2 at a relative humidity of 80%. The i-TE hydrogel demonstrated self-healing behavior, extending its service life. A wearable TE band with twenty devices is prepared to generate a thermovoltage of −2.75 V at a temperature difference of 5.5 K.

5. Improving the Thermopower of i-TE Gels

The i-TE gels are composed of polymers, ions, and solvents, which facilitate six distinct types of interactions: ion-polymer, ion-ion, solvent-polymer, ion-solvent, polymer-polymer, and solvent-solvent interactions.[81–83] Furthermore, the interaction between the electrolyte and the electrodes plays a crucial role in influencing the thermopower of i-TE gels. To achieve further enhancement of the thermopower in i-TE gels, it is essential to develop a comprehensive understanding of the interactions among ions, polymers, solvents, and electrodes, as well as the interactions between the electrolyte and the electrodes.

5.1. Enhancing the Thermopower of p-type i-TE Gels by Structural Engineering and Ion Doping

The thermopower of i-TE gels can be enhanced through structural engineering. The hydrogen bonds within the polymer matrix significantly influence the thermopower of i-TE gels. Chen et al. fabricated PVA/HCl hydrogels that rely on the transport of H^+ ions under a temperature gradient (**Figure 7a**).[67] The H^+

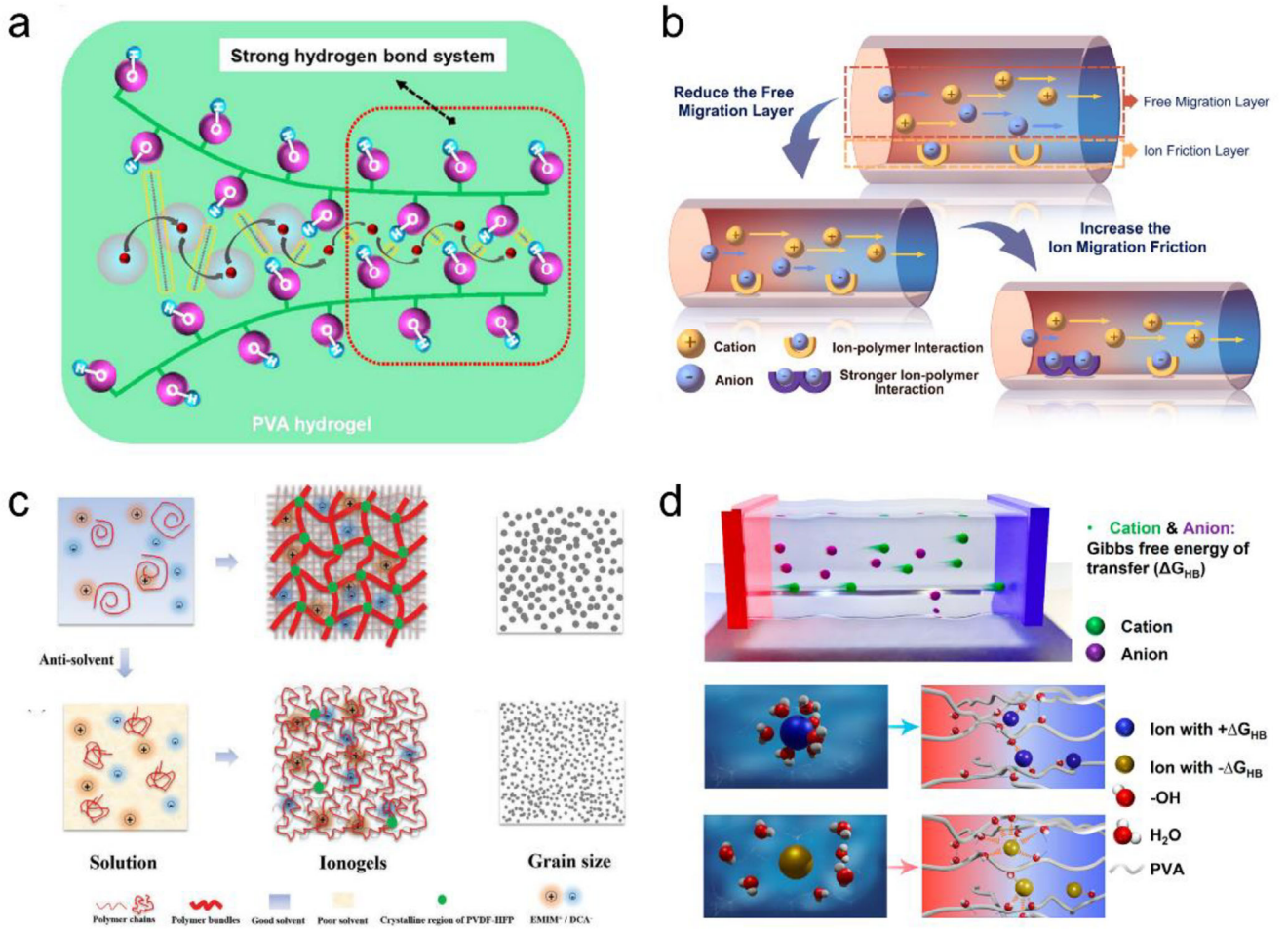

Figure 7. Enhancing the thermopower of p-type i-TE gels. a) Improved thermopower from H^+ movement in a strong hydrogen bonding system. Reproduced with permission.[67] Copyright 2022, American Chemical Society. b) Regulating thermal migration channels improved the thermopower of a cellulose hydrogel. Reproduced with permission.[85] Copyright 2024, Elsevier. c) Solid network engineering significantly enhances thermopower. Reproduced with permission.[36] Copyright 2021, Wiley-VCH. d) A PVA/CsI hydrogel exhibits a thermopower of 52.9 mV K^{-1}. Reproduced with permission.[68] Copyright 2022, American Chemical Society.

cations were introduced into the PVA/HCl hydrogels by swelling the PVA hydrogels with varying degrees of crystallization in the HCl solution. The i-TE gel achieved a remarkable thermopower of 38.2 mV K^{-1} due to the hindering effect of strong hydrogen-bond on anions. Liu et al. investigated the variation in thermoelectric properties induced by the sol-gel phase transition phenomenon in i-TE materials.[84] For the first time, it is reported that there was a substantial increase in thermopower (6.5-folds) and ionic figure of merit (23-folds) in poloxamer/LiCl during the thermally induced sol-gel phase transition. It confirms that the significant enhancement of thermoelectric properties resulting from the phase transition is universal, irrespective of the underlying causes of the sol-gel phase transition. Cheng et al. introduced ionic thermal migration channels for obtaining high ionic thermal power (Figure 7b).[85] The study revealed that channel size and ion interactions are crucial. Initial optimization of the cellulose/KCl hydrogel increased thermal power from 2.45 to 8.13 mV·K^{-1}. Using sodium alginate as the polyanion and multivalent ion crosslinking further enhanced the channel-Cl^- interaction, achieving 22.09 mV·K^{-1}. These cellulose-based i-TE gels are promising for energy harvesting and temperature sensing in wearable devices.

Despite the high thermopower of i-TE gels, their conductivity remained relatively low. The i-TE performance of ionogels composed of PVDF-HFP and EMIM:DCA can be significantly enhanced by engineering the solid network with an antisolvent (Figure 7c).[36] By incorporating ethanol as antisolvent into the ionogel, the polymer grain size decreases, facilitating ion transport along the grain boundaries. The conductivity of the ionogel increased from 7.0 to 17.6 mS cm^{-1} with the addition of 5 wt% ethanol, while maintaining a high thermopower of 25.4 mV K^{-1}. The thermopower can be enhanced by optimizing the microstructure of the i-TE gels. Li et al. synthesized an agarose-based i-TE gel that exhibits a high thermopower of 41.8 mV K^{-1} by decoupling the thermodiffusion of the cation Na^+ and the anion DBS^- (Figure 8d).[86] The incorporation of DBS^- resulted in the formation of a uniform 3D porous structure within the agarose gel, which created ion transport channels facilitating the thermodiffusion of Na^+. The DBS^- anion micelles, characterized by a high density of negative charge, are immobilized within

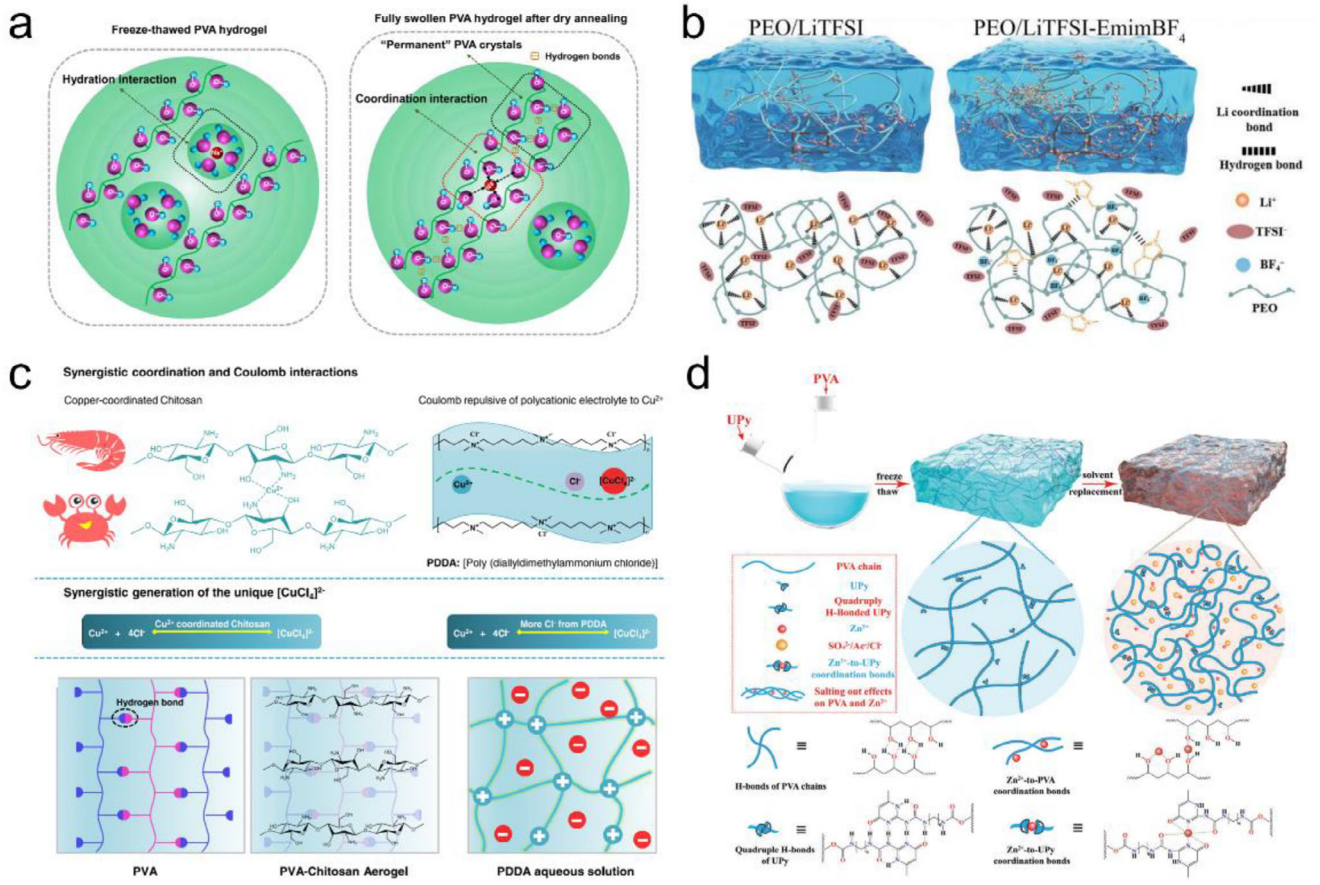

Figure 8. Method for preparing n-type ionogel. a) An N-type ionic hydrogel shows a large negative thermopower via synergistic coordination and hydration. Reproduced under the terms of the CC-BY 4.0 license.[8] Copyright 2021, The Authors, The American Association for the Advancement of Science (AAAS). b) An n-type ionogel with a significant negative thermopower is achieved through metal coordination and ion-selective association. Reproduced under the terms of the CC-BY 4.0 license.[42] Copyright 2023, The Authors, The American Association for the Advancement of Science (AAAS). c) Bidirectionally anchored cations facilitate substantial negative thermopower in multifunctional polymers. Reproduced with permission.[91] Copyright 2023, American Chemical Society. d) An n-type i-TE gel with excellent mechanical properties is fabricated through the synergy of coordination interactions and Hofmeister effect. Reproduced with permission.[92] Copyright 2024, Wiley-VCH.

the polymer matrix, allowing Na^+ cations to move freely within the i-TE gels. Due to the interaction between Na^+ and DBS^- micelles, the Eastman entropy of Na^+ could be increased, thereby enhancing the thermopower. By optimizing the interaction between ions and polymers, Zhao et al. developed an i-TE gel with a high S_i of 18 mV K^{-1} at relative humidity of 60%.[87] The migration of anions is hindered by the hydroxyl groups present in the polymers, while the transport of cations was enhanced through segmental motion, thereby increasing the thermodiffusion difference between cations and anions. Inspired by the rapid cooling of metal alloys for grain refinement and low atomic mobility, Zhang et al. developed a stretchable i-TE gel with a high normalized maximum power density of 2227.5 μW m^{-2} K^{-2} and a thermopower of 4.5 mV K^{-1} through structure engineering induced by liquid nitrogen quenching.[88] The results demonstrate that the nitrogen quenching process can inhibit the crystallization of $[Fe(CN)_6]^{4-}$ and promote a better dispersion of small grains within the hydrogel, thereby increasing the concentration difference of the redox couple between the hot and cold sides.

Ion doping can enhance the thermopower of i-TE gels. Liu et al. developed a novel method to improve thermopower by incorporating sodium dicyanamide (Na:DCA) into an ionogel composed of PVDF-HFP and EMIM:DCA.[35] With the addition of 0.5 mol% Na^+, the i-TE gel exhibits a thermopower of 43.8 ± 1.0 mV K^{-1} at a relative humidity of 85%. The enhancement in thermopower can be attributed to the interactions between the doped Na^+ cations with DCA^- anions, which increase the disparity in the mobilities of $EMIM^+$ and DCA^-. A deeper understanding of the mechanisms underlying ion doping is essential for enhancing the thermopower of i-TE gels. Zhou et al. reported a cationic doping method involving the addition of acetate salts to the ionogels composed of gelatin and EMIM:Ac.[20] An extraordinary thermopower of 37.3 mV K^{-1} is achieved by doping the ionogel with Na:Ac. The enhancement in thermopower is attributed to the lattice energy and melting point of the acetate salts. The study conducted by He et al. offered a novel perspective on the role of ions in i-TE gels.[68] The findings suggest that the capacity of ions to affect hydrogen bonding is a crucial factor. By incorporating

cesium iodide (CsI) into the PVA matrix, the i-TE gels demonstrate a high thermopower of 52.9 mV K^{-1}, which ranks among the largest thermopower values reported to date (Figure 7d). The selection of optimal ion providers can significantly influence the polymer configuration, thereby enhancing the thermopower of i-TE gels. Li et al. introduced a novel strategy that leverages the ion entanglement effect to enhance the thermal diffusion difference between anions and cations.[89] A weak interaction between CF_3SO^{3-} and CH_3SO^{3-}, referred to as anionic entanglement, is confirmed through density functional theory (DFT) calculations. The thermopower 28 mV K^{-1}, and a high output energy density of 67.2 mJ m^{-2} K^{-2} are achieved over a discharge period of 2 h. These findings present a new approach for designing high-performance i-TE gels by manipulating weak interactions among ions.

5.2. Reducing the Thermopower of n-type i-TE Gels by Modulating Ion-Polymer Interactions

In practical applications, the output performance of i-TE gels can be improved by connecting n-type and p-type ionic gels in series. While the thermopower of p-type i-TE gels has achieved a relatively high level, the development of n-type i-TE gels still remain a significant challenge.

Chen et al. developed an i-TE hydrogel with a large negative thermopower through synergistic coordination and hydration interactions (**Figure 8a**).[8] Typically, coordination interactions in i-TE hydrogels are likely to be disrupted by the ion-hydration process. The i-TE gel composed of PVA and sodium hydroxide (NaOH) is prepared using a dry-annealing process followed by a fully swollen process. In this configuration, Na^+ ions can coordinate with PVA polymer chains, while the hydrated OH^- ions serve as the primary thermodiffusion ions in the i-TE gels, resulting in a significant negative thermopower of −37.6 mV K^{-1}. Zhao et al. developed a remarkable n-type ionogel composed of polyethylene oxide (PEO), lithium salt, and ionic liquid (Figure 8b).[42] To enhance anion transport and increase transfer entropy, they propose a strategy that leverages metal-ligand coordination in conjunction with ion-selective association. Molecular dynamics simulations confirm that the presence of anion clusters and preferential ion association significantly facilitate anion diffusion. This enhancement has resulted in high i-TE performance, characterized by a thermopower of −15 mV K^{-1} and an ionic conductivity of 1.86 mS cm^{-1} at a relative humidity of 50%. The i-TE gels exhibit excellent stretchability and self-healing properties, attributed to the dynamic and reversible physical crosslinking between lithium ions and the ether oxygens of PEO chains. Additionally, the i-TE gels demonstrate exceptional recyclability, as they can be dissolved in ethanol and regenerated through solvent evaporation.

The thermopower of p-type i-TE gels has reached a relatively high level. However, the development of n-type i-TE gels with comparable performance remains a significant challenge. Le et al. introduced a synergistic doping method to convert p-type i-TE gels into n-type.[90] By incorporating Ag^+ and OTf^-, Ag^+ forms a complex with $BMIM^+$, while OTf^- interacts strongly with $BMIM^+$. This interaction retards the migration of $BMIM^+$ cations and increases the thermodiffusion difference between $BMIM^+$ and BF_4^-. The resulting n-type i-TE gel achieved a high thermopower of −26.4 mV K^{-1} under a relative humidity of 75%. The interactions between ions and polymers play a critical role in the development of hydrogels with high i-TE performance. Further investigation into various types of interactions is necessary to enhance i-TE performance. Chen et al. explored the synergistic applications of two different types of interactions in i-TE materials (Figure 8c).[91] The i-TE hydrogel is prepared by infiltrating a $CuCl_2$-PDDA solution into a PVA-chitosan aerogel, resulting in high i-TE performance (S_i = −28.4 mV K^{-1}) at room temperature. The significant negative thermopower arises from the coordination interactions between Cu^{2+} and chitosan, as well as the Coulomb repulsion of Cu^{2+} by the polycationic PDDA polymer. This interaction facilitates the transport of anions presented by $[CuCl_4]^{2-}$. The $[CuCl_4]^{2-}$ ions, characterized by their unique hydration structure, are prevalent in aqueous $CuCl_2$ solutions and exhibit a higher thermodiffusion speed compared to Cl^-. In the i-TE gels, both the confinement of Cu^{2+} by chitosan and the abundance ionizable Cl^- in PDDA can synergistically promote the synthesis of $[CuCl_4]^{2-}$. The critical role of $[CuCl_4]^{2-}$ in the development of n-type i-TE gels has not yet been fully understood.

For practical applications, it is essential to fabricate n-type i-TE gels with outstanding mechanical properties. Hu et al. demonstrated multi-hierarchical network-enhanced i-TE gels that exhibited simultaneously improved thermoelectric and mechanical performance (Figure 8d).[92] By immersing the PVA organogel in specific ionic salt solutions, both coordination interactions and the Hofmeister effect are achieved. The mobility of anions is enhanced due to the coordination interactions and the salting-out effect. The PVPy30-1.5 combines exceptional mechanical properties with high TE performance, including remarkable tensile strength (>6.7 MPa) and toughness (>43 MJ m^{-3}), along with significant negative thermopower (−3.6 mV K^{-1}) at room temperature.

5.3. Bidirectional Modulating the Thermopower of i-TE Gels through Multiple Strategies

In practical applications, the output voltage of i-TE devices can be improved by connecting n-type and p-type cells in series. By modulating the interactions between ions and polymers, ions and ions, or ions and electrodes, the thermopower of i-TE gels can be adjusted from p-type to n-type, thereby enhancing the overall output performance of the gels (**Figure 9**).

Previous efforts have focused on ion-matrix interactions to modulate the i-TE properties. Here, Liu et al. proposed a novel strategy to enhance the thermopower by leveraging strong ion-ion interactions in ternary polymer gels (**Figure 10a**).[93] By incorporating of ion salts into the ternary ionogels, the thermopower can be adjusted from −15 to 17 mV K^{-1}. By appropriately selecting the doping salts that interact with either cations or anions, the dominant diffusion ions in the ternary ionogels can be precisely controlled, allowing for tailored thermopower. A wearable i-TE device with 12 pairs of p/n legs was fabricated, exhibiting a thermopower of 0.358 V K^{-1}. Ion salts can be utilized as thermopower regulators to create a bipolar i-TE gels. Liu et al. developed a stretchable and self-healing ionogel with bipolar thermoelectric properties.[94] By substituting the salt from

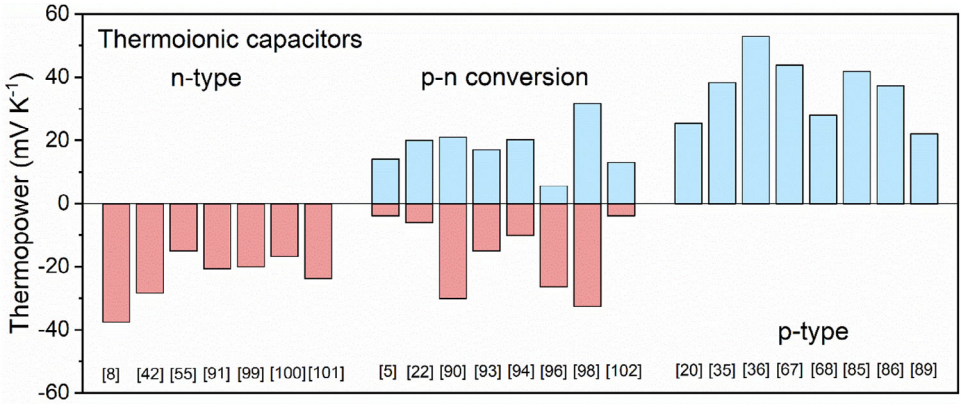

Figure 9. Thermopower of the thermoionic capacitors made from n-type,[8,42,55,91,99–101] from n-type to p-type,[5,22,90,93,94,96,98,102] and p-type i-TE gels.[20,35,36,67,68,85,86,89]

EMIM:Cl to $LiBF_4$, the thermopower of the ionogels varies from −21 to 30 mV K^{-1}. The ionogel exhibits a robust self-healing capability due to strong ion-dipole interactions. A flexible thermoelectric detector, consisting of ten pairs of p/n legs, demonstrates a thermovoltage of 0.25 V K^{-1} with a temperature difference of 1–2 K. Zhao et al. demonstrated ambipolar i-TE gels with a tunable thermopower by adjusting the gel composition (Figure 10b).[5] The magnitude and sign of the thermopower in the i-TE gels can vary from −4 to 14 mV K^{-1} with the addition of liquid neutral PEG. The interaction between ions and polymers plays a central role in modulating the thermopower, as the dominating thermodiffusion ions transition from anions to cations. The solution processability of the i-TE gels facilitates screen printing and the large-scale fabrication of the thermopiles at a low cost. A thermosensitive i-TE module with 18 pairs of connected thermocouples generates a thermopower of 0.333 V K^{-1}. Here, Duan et al. developed a novel system that facilitates p-n conversion for the iodide/triiodide (I^-/I_3^-) redox couple, induced by thermosensitive PNIPAM nanogels (Figure 10c).[3] The PNIPAM nanogels possess a low critical solution temperature (LCST, ≈32 °C), exhibiting a hydrophilic state at low temperatures and transitioning to a hydrophobic state at elevated temperatures. The i-TE gels can be converted from p-type (S_i = 0.7 mV K^{-1}) to n-type (S_i = −1.9 mV K^{-1}) with the incorporation of PNIPAM nanogels. This conversion of the thermopower occurs as the nanogels capturing I_3^- at the hot side and release I^- at the cold side, thereby creating a concentration gradient of I^- across the thermocell. A wearable device has been designed with consideration from the transition temperature of the nanogels, which is approximately equal to body temperature. This device generates an output voltage of 1 V by harnessing body heat. Guo et al. utilized the rapid and reversible pH shift of a solution containing temperature-responsive hydrogel nanoparticles, resulting in a thermocell with a high S_i at approximately room temperature.[95] At physiological temperatures, the thermocell achieves a high S_i due to the swift and reversible pH shift of the temperature-responsive hydrogel nanoparticles. The concept of entropy-driven phase transitions in hydrogel nanoparticles presents a novel approach for developing nontoxic, high-performance thermocells.

Zhao et al. demonstrated self-healing and robust ionogels with tunable thermoelectric properties through metal-halogen bonding interactions (Figure 10d).[96] The ionic conductivity and mechanical strength of the ionogels are simultaneously enhanced by introducing phase separation between the polymer matrix and the salts in the ternary PEO/LiTFSI/EMIM:Cl ionogel. The dominant transport ions shift from anions to cations with the addition of EMIM:Cl, resulting in a transition from n-type to p-type behavior in the i-TE gels within the same polymer matrix. The thermopower of the ternary ionogel can be adjusted from −4 to 13 mV K^{-1} while maintaining its self-healing capability. By controlling the phase transition process, tunable i-TE performance in thermoelectric devices can be achieved for low-grade heat harvesting applications.

Through the use of i-TE hydrogels for low-grade heat harvesting, their mechanical and thermal stability is often inadequate. Kim et al. reported a side-chain engineering strategy to develop p-type and n-type ionic gels that exhibit stretchability and self-healing properties (Figure 10e).[97] The polymer, designed with long ionic side chains, facilitates the passage of a single ion species, resulting in a thermopower that varies from 5.8 to −4.2 mV K^{-1}. The i-TE devices, which incorporate five pairs of p/n thermocouples, demonstrate a high thermovoltage of ≈0.8 V. Controlling the thermodiffusion behavior of cations and anions is essential for achieving high-performance i-TE materials. Lee et al. utilized pH-sensitive zwitterionic (ZI) polymers to achieve bipolar properties by manipulating the environmental pH (Figure 10f).[98] By immersing the ZI hydrogel in various aqueous solutions with pH levels ranging from 1 to 14, the thermopower varies from −32.6 to 31.7 mV K^{-1}. This research presents a straightforward strategy for fabricating bipolar i-TE gels through the adjustment of environmental pH.

Chi et al. demonstrated reversible bipolar thermopower using the same i-TE gels by modulating the ion-electrode interactions (Figure 10g).[22] The thermopower of the i-TE device transitioned from p-type (20.2 ± 4 mV K^{-1}) to n-type (−10.2 ± 0.8 mV K^{-1}) when the electrode is switched from copper to amorphous carbon nanotubes. The interfacial interactions and the polarization arrangement of ions vary significantly with different electrodes. By alternating the external electrodes, the i-TE gel is able to achieve cyclic power generation under constant thermal conditions. The approach of changing electrode, rather than altering the thermal contact between materials and heat or re-establishing

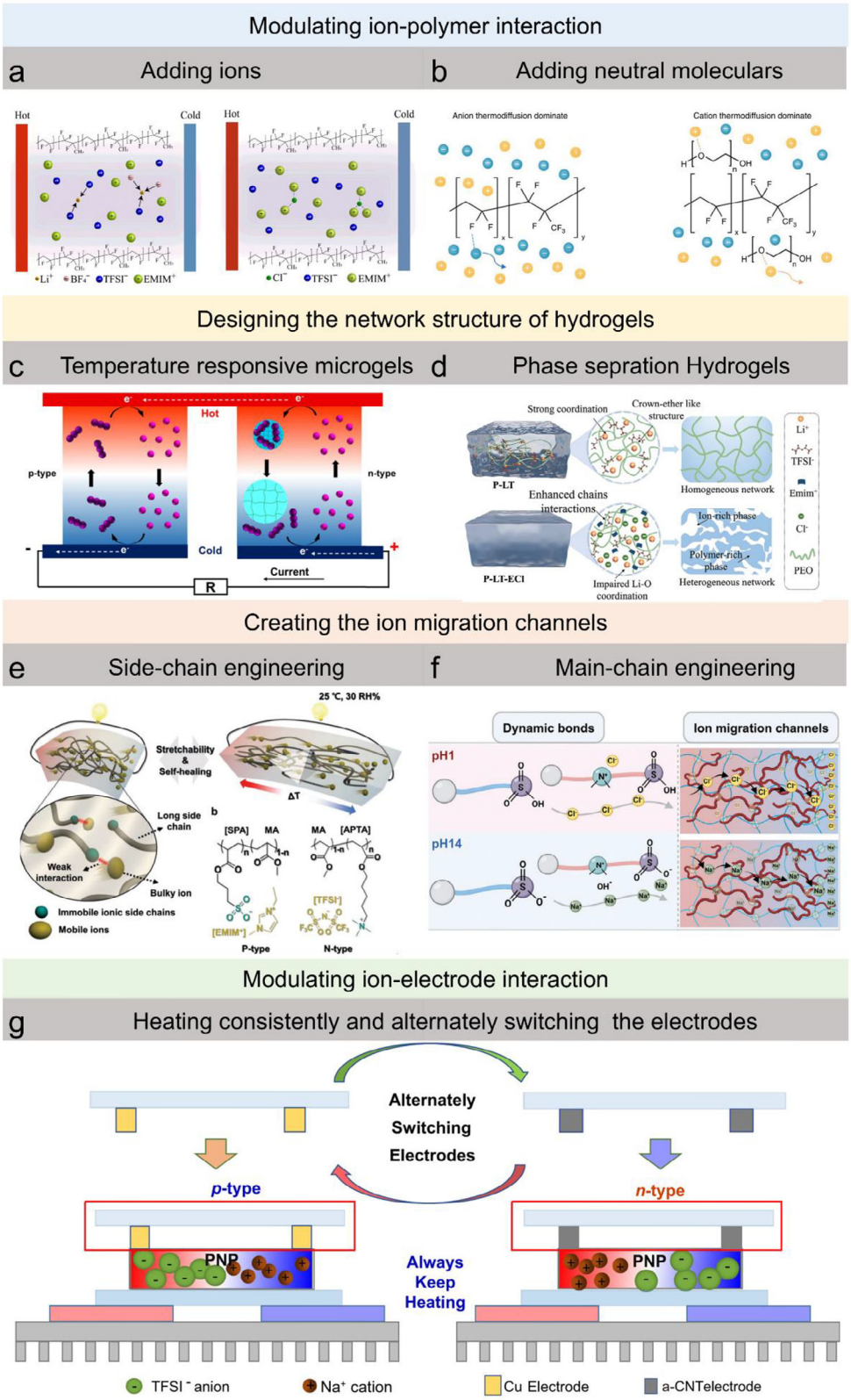

Figure 10. Methods for converting p-type ionogel to n-type ionogel. a) Bidirectional modulation of the thermopower in i-TE gels enabled by selective ion doping. Reproduced under the terms of the CC-BY 4.0 license.[93] Copyright 2022, The Authors, The American Association for the Advancement of Science (AAAS). b) An ambipolar i-TE gel with tunable thermopower has been developed by adjusting the gel composition. Reproduced under the terms of the CC-BY 4.0 license.[5] Copyright 2019, The Authors, Springer Nature. c) P-N conversion for the iodide/triiodide (I^-/I_3^-) redox couple induced

the temperature difference, can enhance the efficiency of i-TE generators.

6. Improvement on the Thermoelectric Output Performance of i-TE Gel-based Device

Despite the various methods been applied to improve the thermopower of i-TE gels, the output performance of a single i-TE gel remains limited and does not meet the requirements for practical applications. I-TE gel-based devices, like thermoelectric modules can be fabricated by connecting multiple i-TE gel cells. Therefore, it is imperative to further enhance the output performance of i-TE gel-based devices.

6.1. Optimal Design of the Electrodes and Electrolytes

Given that the interaction between the electrode and the electrolyte enhances the thermopower of the ionic gel, the thermoelectric output of the ionic gel can be improved by optimizing the microstructure of the electrode. By developing a 3D hierarchical structure for the electrode, the maximum power density of the i-TE cells based on synergistic effect can be increased due to the enhanced thermogalvanic reaction sites and the reduced interfacial charge transfer resistance (**Figure 11a**).[9]

Despite the potential of thermocells for harvesting low-grade heat, their power density and energy conversion efficiency of thermocell are often hindered by low conductivity and a narrow operational window of the electrolyte. Li et al. developed an anti-freezing thermocell system with anisotropic holey graphene aerogel as electrodes, enabling operation across a wide temperature range (Figure 11b).[103] The anisotropic holey graphene aerogel exhibits remarkable ion conductivity due to its aligned graphene sheets and pores. The eutectic electrolyte, characterized by high ion conductivity, is prepared by mixing formamide and water, significantly increasing the operational temperature range from 0 to −40 °C. A single thermocell was fabricated by assembling the anisotropic graphene aerogel electrode with the eutectic electrolyte, demonstrating a high maximum power density of 3.6 W m^{-2} and a thermopower of 1.3 mV K^{-1}. The output voltage of the assembled thermocells increased form 140 mV (for a single-cylinder thermocell) to 2.1 V (for fifteen-cylinder thermocells).

Currently, i-TE gels exhibit suboptimal performance in terms of i-TE potential, output power density, and energy density, which limits their practical use. While optimizing gel composition can enhance performance, effective strategies are limited. Niu et al. introduced the concept of "high entropy" into i-TE gels, developing high-entropy gel thermoelectric batteries that exhibited excellent performance near room temperature (Figure 11c).[104] The high-entropy structure, formed through multi-anion coupling, significantly increased the entropy change of the redox reaction, exchange current density, and ionic conductivity, enhancing energy collection. After 50 cycles of quasi-continuous discharge, the high-entropy i-TE gel maintained a stable voltage of 95 mV at a ΔT of 3 K for up to 250 min, demonstrating good stability and a long lifespan suitable for practical battery applications. Niu et al. developed an ion thermoelectric-electrochemical (i-TE-EC) thermocell using two types of asymmetric gels to form a double sandwich structure (Figure 11d).[105] The integration of electrochemical energy significantly enhances thermoelectric conversion performance, attributed to the synergistic effect based on thermodiffusion effect and thermogalvanic effect of the asymmetric gels. By optimizing the gel composition through adjustments in the concentration and ratio of redox materials and the content of additives, the thermoelectric performance of the i-TE-EC battery was further improved. A gel device composed of nine i-TE-EC thermocells connected in series achieved an output voltage of 1.55 V and a normalized maximum power density of 5.2 mW m^{-2} K^{-2} at 40 °C. Additionally, Zhang et al. prepared an anti-freezing, stretchable thermocell based on thermogalvanic effect by introducing guanidine ion-induced $[Fe(CN)_6]^{4-}$ ion crystallization.[48] This thermocell exhibits high thermoelectric performance, with a remarkable thermopower of 4.4 mV K^{-1} and a record-high normalized output power density of 1780 μW $m^{-2}K^{-2}$. By generating a stable voltage and reducing the CPU temperature by 1.5 K, this thermocell demonstrates that thermal management and power generation can be achieved simultaneously.

6.2. Hybrid Working Mode

A temperature difference application-removal cycle is necessary to facilitate the charging and discharging processes of i-TE generator, which can be time-consuming and inefficient. Achieving a continuous power supply while maintaining a constant ΔT through the design of the electrolyte structure presents significant challenges.

Currently, i-TE gels are utilized in a capacitive mode, as ions cannot enter the external circuit, resulting in a discontinuous working mode and low energy density. He et al. demonstrated a continuous output by converting the ionic current into electrical current using an ion-electron conductor(Figure 11e).[106] The i-TE devices based on the ion-electron conductors can directly power electronic devices. A porous carbonized pomelo peel filled with ionic liquid is designed to facilitate the transport of both ions and electrons. When a temperature gradient is applied to the i-TE gel, an electric field was established due to the Soret effect. As electrons pass through the i-TE gel, a portion of the drift current can flow through the external circuit, resulting in a continuous operating mode that converts ionic current into electrical current. A large p-type thermopower of 11.58 mV K^{-1} was achieved by combining the coupling effect of thermodiffusion and

by poly(N-isopropylacrylamide) (PNIPAM) thermosensitive nanogels. Reproduced with permission.[3] Copyright 2019, Elsevier. d) A self-healing and durable ionogel with tunable thermoelectric performance is developed through phase separation induced by metal-halogen interactions. Reproduced with permission.[96] Copyright 2024, Wiley-VCH. e) P-type or n-type i-TE gels with long ionic side chains that exhibit tunable i-TE performance. Reproduced with permission.[97] Copyright 2023, Wiley-VCH. f) A pH-sensitive zwitterionic hydrogel with a double network structure that demonstrates bipolar thermoelectricity. Reproduced with permission.[98] Copyright 2024, Wiley-VCH. g) Reversible bipolar thermopower of i-TE gels through manipulation of the interactions between ions and electrodes. Reproduced under the terms of the CC-BY 4.0 license.[22] Copyright 2023, The Authors, Springer Nature.

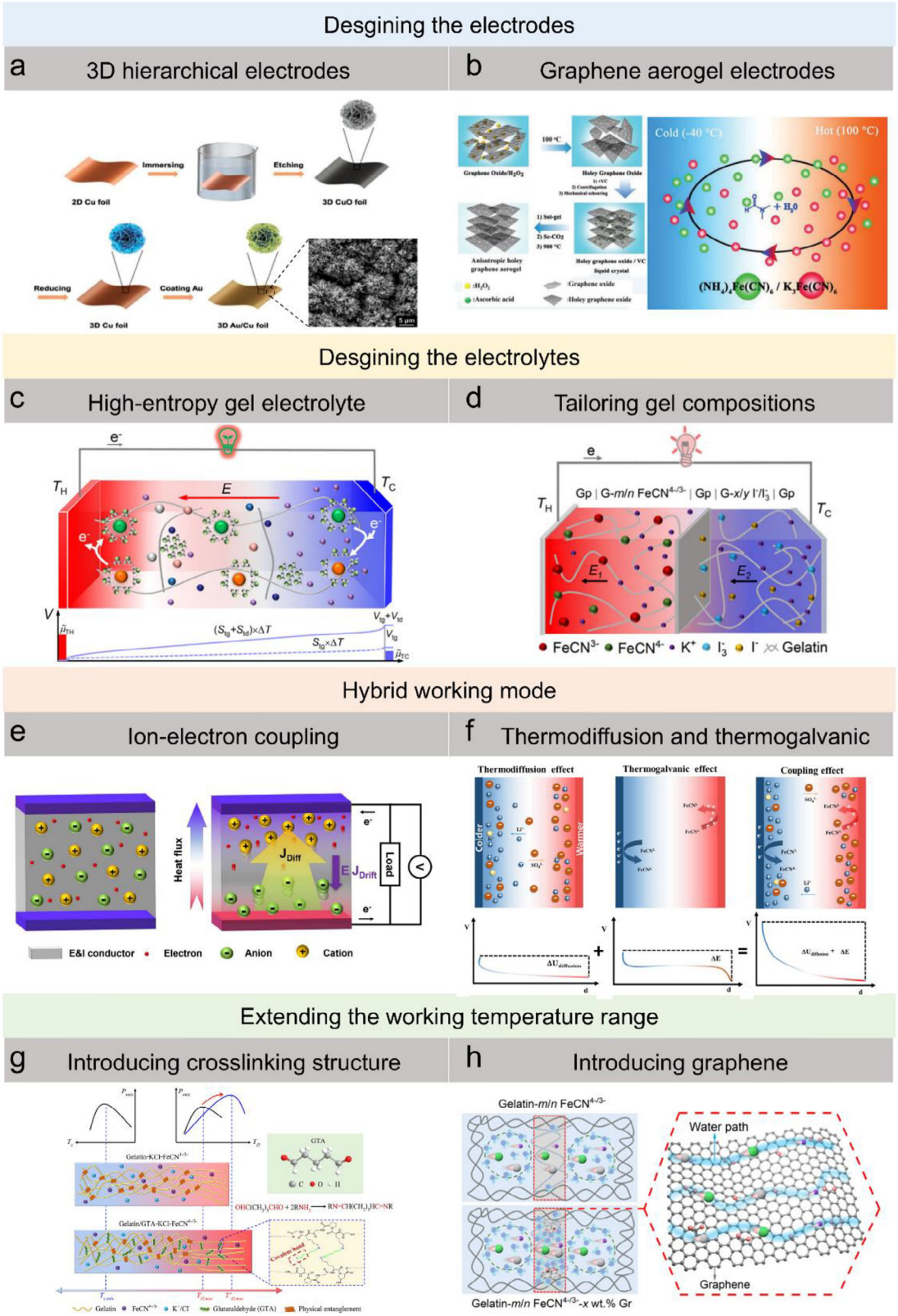

Figure 11. Enhancing the thermoelectric output performance of i-TE gels. a) Ultrahigh power output from i-TE thermocells with 3D hierarchical electrodes. Reproduced with permission.[9] Copyright 2022, Wiley-VCH. b) An electrochemical thermocell with high i-TE performance uses anisotropic holey graphene aerogel electrodes and a eutectic redox electrolyte. Reproduced with permission.[103] Copyright 2019, Wiley-VCH. c) Remarkable i-TE performance achieved by a high-entropy gel electrolyte. Reproduced with permission.[104] Copyright 2025, Royal Society of Chemistry. d) An i-TE-EC thermocell

thermogalvanic effect (Figure 11f).[107] The i-TE gel with superior stretching and adhesion property can output an energy density of 32 mW m^{-2} at a temperature gradient of 15 K. Wang et al. reported that thermoelectric conversion efficiency can be enhanced by combining the Soret effect with the proton-coupled electron transfer (PCET) reaction of benzoquinone and hydroquinone.[108] An energy storage function can be achieved through the redox couple, maintaining a power output of 27.7% and 14 mW m^{-2} for over 3 h by rebalancing the PCET reactants in the hydrogel. Jiang et al. developed an i-TE generator with high energy density by harnessing the synergy between the thermodiffusion effect and the redox reactions occurring at the electrodes.[23] The i-TE gel exhibited a notable thermopower of 40.6 mV K^{-1}, which can be attributed to the phase transition behavior induced by hydrogen bonding during heating. Furthermore, the i-TE gel, when combine with a polyaniline (PANI) electrode, can function as a continuous and recyclable power source.

6.3. Extending the Working Temperature Range

Currently, the i-TE gel-based thermocells exhibit a relatively low output power density. The limited operational temperature range restricts the potential for further enhancement of this output power density. A flexible i-TE gel-based thermocell has been developed by incorporating glutaraldehyde into the gelatin-KCl-$FeCN^{4-}/^{3-}$ matrix, significantly improving the thermal stability of the gel (Figure 11g).[109] The maximum temperature differential has been increased from 9 to 23 °C. The gelatin/glutaraldehyde polymer network enhances the entropy difference of the $FeCN^{4-}/^{3-}$ redox couple, thereby improving its thermoelectric power. A flexible and wearable device composed of 16 i-TE cells can generate a high voltage of 3.6 V and an output power of 115 mW by harnessing body heat.

The i-TE performance of thermocells was limited by the restricted thermal tolerance of i-TE gels. Han et al. developed a strategy to enhance the thermopower and output power density by incorporating graphene into i-TE gels (Figure 11h).[110] Graphene improves the i-TE performance of thermocells by forming a bridge-like structure. The i-TE gel demonstrated a high thermopower of 13 mV K^{-1} at 323 K. A record-high normalized maximum power density of 1.2 mW m^{-2} K^{-2} is achieved at 323 K by connecting four thermocells in series.

6.4. Enlarging the Temperature Difference

In the case of thermionic capacitors and thermocells, the normalized maximum power density ($P_{max}A^{-1}\Delta T^{-2}$, where P represents the maximum power output and A denotes the module's cross-sectional area) is at least one order of magnitude lower than that of thermoelectric devices. The primary reason for the reduced power density is the significant internal resistance of thermionic capacitors, combined with the weak driving force provided by the temperature difference. The temperature difference acts as the driving force for the i-TE generator, and the output performance of the i-TE generator can be enhanced by increasing the temperature difference through methods such as radiative cooling or evaporative cooling. Furthermore, the ionic gels can be employed for thermoelectric energy generation and freshwater collection, thereby improving the efficiency of energy and water conversion.

Yang et al. developed a self-sustaining thermocell based on thermogalvanic effect in conjunction with a passive radiative cooling layer (**Figure 12a**).[11] The thermogalvanic ionogel is composed of a poly(N,N-dimethylacrylamide) (PDMAA) network, an ionic liquid (EMIM:DCA), and ion redox couple ($[Fe(CN)_6]^{4-}/[Fe(CN)_6]^{3-}$). This ionogel demonstrates a remarkable thermopower of 32.4 mV K^{-1} and maintains stable thermoelectric performance over a broad temperature range (≈−40–90 °C), enabling effective energy harvesting under diverse weather conditions. A thermoelectric module is constructed by integrating 80 units, yielding an output voltage exceeding 45 V under a solar intensity of 1000 W m^{-2}.

Traditional semiconductor thermoelectric devices struggle to dissipate heat effectively during low-grade heat harvesting, leading to decreased efficiency in core energy conversion systems. To tackle this issue, Liu and colleagues have developed a smart thermoelectric hydrogel by combining low-grade heat harvesting and evaporative cooling (Figure 12b).[111] The redox reactions of ions within the hydrogel, along with moisture evaporation and absorption, create two independent thermodynamic cycles. This innovative approach allows for efficient evaporative cooling while thermoelectric conversion occurs. When applied to a heating element, the hydrogel film can convert waste heat into electrical energy, while the moisture rapidly evaporates to dissipate heat, thereby lowering the device's temperature. Additionally, when not in use, the hydrogel film absorbs moisture from the air, enabling spontaneous recycling. High temperatures generated during the rapid charging and discharging of high-power batteries can pose safety risks. A 2 mm-thick thermoelectric hydrogel film reduce the temperature of a mobile phone battery by 20 °C during rapid discharge, while also recovering energy for self-monitoring and system control.

6.5. Assembling of Thermoelectric Modules

Generally, the output voltage of a single i-TE device operates at the millivolt level. Furthermore, the power density of thermionic capacitors and thermocells is lower than that of thermoelectric devices, which presents challenges for practical applications. However, due to the solvent processing characteristics of i-TE gels, they can be printed on a large scale to fabricate thermoelectric modules. These thermoelectric modules can harness energy

employs two types of asymmetric gels to form a double sandwich structure. Reproduced with permission.[105] Copyright 2024, Royal Society of Chemistry. e) High-performance i-TE materials are designed through ion-electron thermoelectric interactions. Reproduced under the terms of the CC-BY license.[106] Copyright 2023, The Authors, Springer Nature. f) Double network i-TE gels enhance performance by combining thermodiffusion and thermogalvanic effects. Reproduced with permission.[107] Copyright 2023, Elsevier. g) Record-high output power in gelatin-based i-TE gels achieved by extending the operational temperature range. Reproduced with permission.[109] Copyright 2022, Royal Society of Chemistry. h) Thermopower and maximum power density improved at elevated temperatures with graphene incorporation.[110] Reproduced with permission. Copyright 2024, Royal Society of Chemistry.

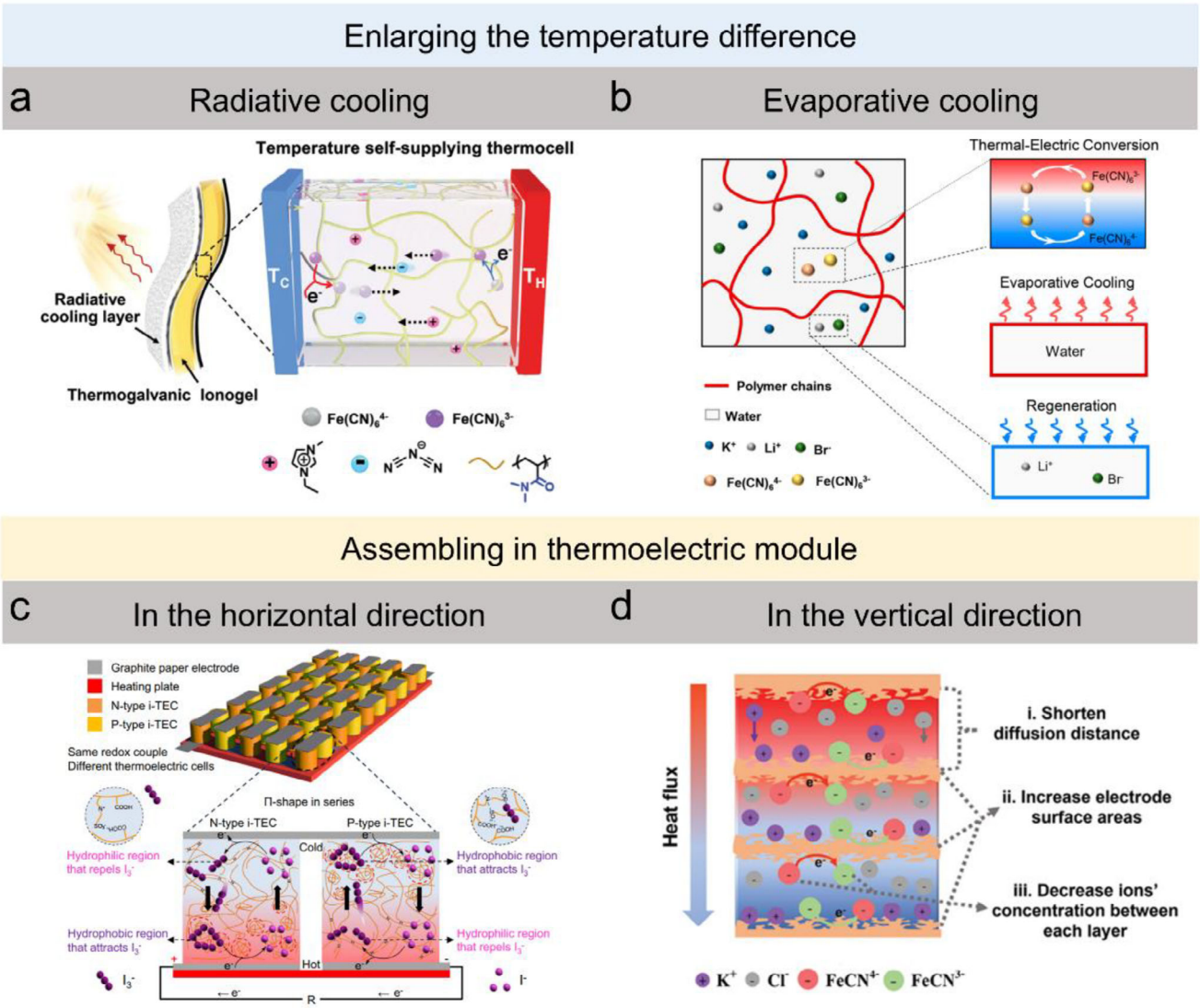

Figure 12. Enhancing the output performance of i-TE gels. a) Showcasing integrated chaotropic effect-enhanced thermocells as practical power sources. Reproduced with permission.[11] Copyright 2024, Wiley-VCH. b) Smart i-TE gels for low-grade heat harvesting and evaporative cooling. Reproduced with permission.[111] Copyright 2020, American Chemical Society. c) A high-performance thermoelectric module integrates n-type and p-type i-TE gels in series. Reproduced under the terms of the CC-BY license.[112] Copyright 2024, The Authors, Springer Nature. d) Connecting multiple electrodes in series reduce thermal charging time and increase output energy density of thermocells.[24] Reproduced with permission. Copyright 2024, Wiley-VCH.

from the surrounding environment, providing sufficient electricity to power various electronic devices.

A stretchable thermocell for wearable power supply by combining a polyacrylamide (PAAm) matrix with different redox ion pairs.[43] The thermopower of the n-type and p-type ionogels is −1.46 and 1.38 mV K^{-1}, respectively. The i-TE gel conforms to the curved surface of the arm while maintaining its thermoelectric properties, demonstrating its potential for use in stretchable wearable devices. By integrating a graphite paper electrode, a body-conformal and portable thermocell device is created, producing a voltage output of 0.16 V from 14 pairs of p-n junctions.

Xia et al. demonstrated that p-n conversion in thermocell can be achieved through the phase transition of temperature-sensitive hydrogels with triiodide/iodide redox pairs (Figure 12c).[112] The interaction between triiodide and the hydrogel's hydrophobic region captures triiodide on the hydrophilic side while repelling it on the hydrophobic side, increasing the concentration gradient and enhancing the thermopower. The n-type thermocell exhibits a thermopower of 7.7 mV K^{-1}, whereas the p-type thermocell has a thermopower of −6.3 mV K^{-1} (ΔT = 15 K). Connecting 10 pairs of p-n junction yielded a voltage of 1.8 V and an output power of 85 μW, surpassing previous reported thermocells. This work introduces a phase transition strategy for p-n conversion and emphasizes the potential of integrated thermocells for low-grade heat energy harvesting.

I-TE gel-based thermocells encounter challenges such as extended thermal charging times and low output power. Liu et al.

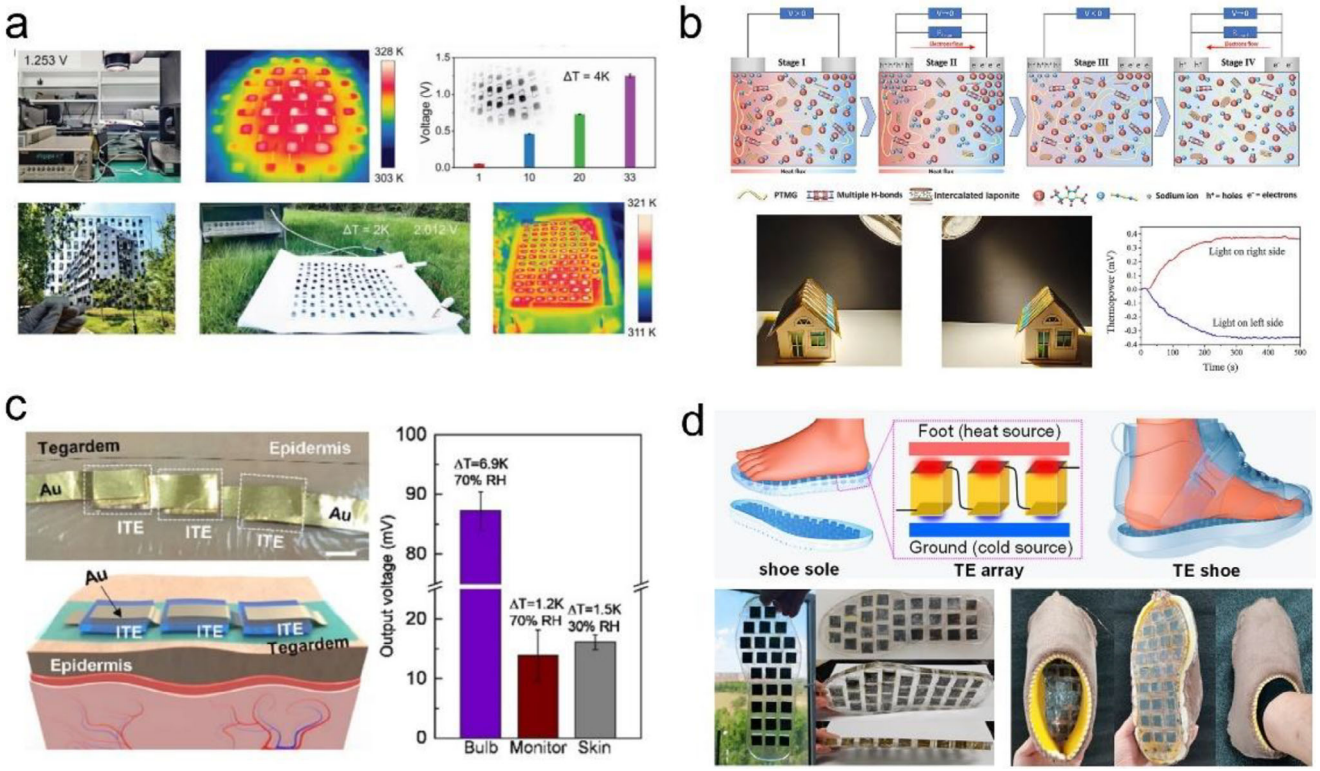

Figure 13. i-TE gels for low-grade heat harvesting. a) Mechanically adaptive, waterproof i-TE gels for energy harvesting. Reproduced under the terms of the CC-BY license.[113] Copyright 2023, Wiley-VCH. b) Nanocomposite ionogel thermionic capacitors for solar-to-electricity conversion. Reproduced with permission.[14] Copyright 2022, The Authors, Springer Nature. c) Stretchable ionic thermoelectric supercapacitors for wearable heat harvesting. Reproduced with permission.[47] Copyright 2023, Elsevier. d) Wearable thermoelectric shoes with antifreezing hydrogels for heat harvesting in ultralow temperatures. Reproduced with permission.[76] Copyright 2023, American Chemical Society.

introduced a multilayer electrode design that reduces ion diffusion distance and increases electrode surface area, significantly decreasing thermal charging times (Figure 12d).[24] Increasing the number of electrode layers from 2 to 8 reduced the charging time from 27 min to just 8 min. The i-TE battery showed excellent cycling stability, with 2 h output energy density of 403 J m^{-2} was achieved over 7 cycles. A flexible, wearable i-TE device consisting of 20 units generated 3.8 V and 282 μW by harnessing body heat. This research offers a promising approach to enhance the applications of i-TE device in power generation.

7. Applications of i-TE Gels

7.1. Arrayed/Wearable Devices based on i-TE Gels for Low-Grade Heat Harvesting

Converting waste heat from buildings and the environment into electricity can help mitigate the energy and environmental crisis. By replacing traditional building coatings with thermoelectric coatings, waste heat generated by buildings can be harvested and transformed into electricity. Zhao et al. developed a high-performance i-TE gel featuring a high n-type thermopower of −8.8 mV K^{-1} based on synergistic ionic associations (**Figure 13a**).[113] Furthermore, the i-TE gel demonstrates excellent adaptability to irregular surfaces, a rapid self-healing capability (120 s), and remarkable stability under harsh environmental conditions. The i-TE gels can be applied to the roof of a model building to create a planar temperature gradient. Even on a cloudy day, the open-circuit thermovoltage for a painted i-TE array with an area of ≈8.5×10^{-3} m^2 exceeds 2 V.

Xiao et al. reported a durable and stretchable nanocomposite ionogel created by incorporating ionic liquid and Laponite nanosheets into a WPU polymer matrix (Figure 13b).[14] The presence of multiple hydrogen bonds in WPU enables the ionogel to accommodate a higher concentration of ionic liquid, thereby enhancing its conductivity. Furthermore, the ionogel demonstrates a high thermopower of 44.1 mV K^{-1} and a low thermal conductivity of 0.43 W m^{-1} K^{-1} due to the inclusion of Laponite. This nanocomposite ionogel can be fabricated into a thermoelectric capacitor, enabling the conversion of heat from solar radiation into electricity.

The softness and adaptability of i-TE gels enable them to closely conform to the human body and accommodate its movements. Compared to traditional thermoelectric materials, i-TE gels have lower thermal conductivity, which helps maintain a consistent temperature gradient essential for effective energy conversion. Park et al. presented a fully stretchable ITESCs by sandwiching the i-TE gel between two Au-TiO_2 nanowire (NW)/thermoplastic polyurethane (TPU) electrode layers (Figure 13c).[47] The i-TE gel composes of a polyethylene diacrylate (PEGDA)/2-hydroxyethyl acrylate (2-HEA) network and a non-volatile ionic liquid (EMIM:TFSI). This gel exhibits a high

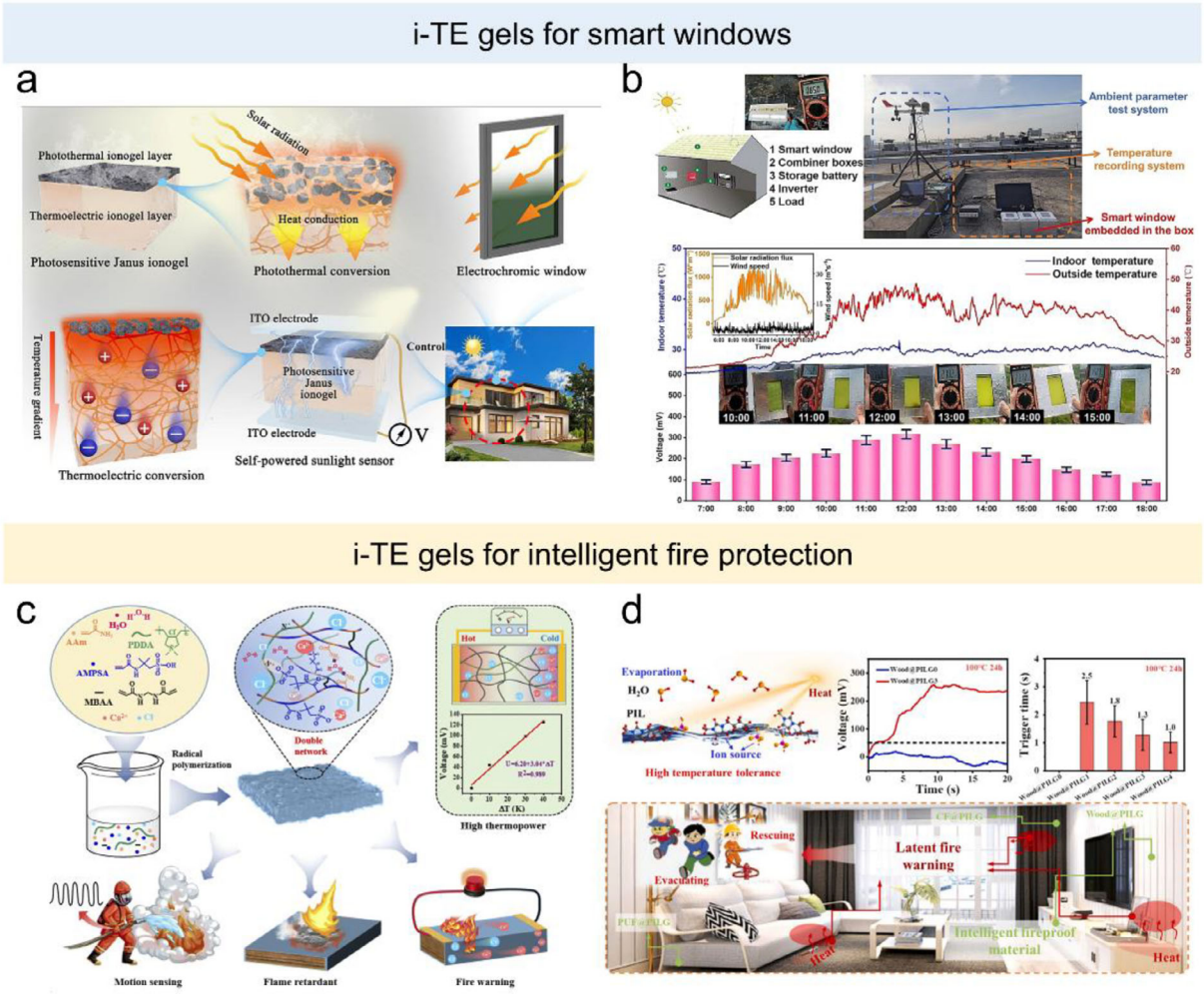

Figure 14. i-TE gels for thermal sensing applications. a) Photosensitive Janus ionogel converting solar energy to electricity. Reproduced with permission.[15] Copyright 2024, Elsevier. b) Dual-module smart window with a thermochromic hydrogel for temperature regulation and electricity generation. Reproduced with permission.[114] Copyright 2024, Elsevier. c) A flame-retardant ionic hydrogel with high thermopower and sensitive fire warnings. Reproduced with permission.[115] Copyright 2022, Royal Society of Chemistry. d) Self-powered fire protection ionogels with accurate temperature sensing. Reproduced with permission.[116] Copyright 2024, Elsevier.

thermopower of 38.9 mV K^{-1} at a relative humidity of 90%. This gel demonstrated reliable mechanical stability at 50% strain over 500 repetitive cycles. Zhang et al. reported anti-freezing thermogalvanic hydrogels for body heat harvesting at ultralow temperature environment (Figure 13d).[76] The i-TE gel displays excellent anti-freezing properties due to the formation of hydrogen bonds between ethylene glycol and free water molecules. This i-TE gel can enable self-powered breath monitoring and bi-directional communication using Morse code. Additionally, a wearable thermoelectric shoe has been developed by integrating the i-TE gel into the shoe, allowing it to harvest body heat even in cold conditions, down to −30 °C.

7.2. i-TE Gels for Smart Windows and Intelligent Fire Protection

Sun et al. reported a photosensitive Janus ionogel with pseudo-photoelectric efficiency based on cascade conversion, exhibiting a thermopower of 19.5 mV K^{-1} (**Figure 14a**).[15] The photosensitive Janus ionogel is synthesized through in situ polymerization of the thermoelectric ionogel on the photothermal layer. Through the "light-thermal-electric" cascade conversion process, the photosensitive Janus ionogel can generate electricity by converting solar energy. This ionogel demonstrated a maximum volume energy density of 2.6 J m^{-3} when harnessing solar energy.

With the capability to intelligently adjust color and light transmittance, thermochromic smart windows have gained significant attention for their potential to enhance energy efficiency in buildings and improve residential comfort. Xie et al. introduced an intelligent solar thermal utilization window composed of PNIPAmgly5 thermochromic hydrogel and PVA-based thermoelectric hydrogels (Figure 14b).[114] When exposed to sunlight, the thermochromic hydrogel exhibits a sunlight shielding rate of up to 99.2%, effectively reducing excessive solar energy from entering the room. Additionally, the PVA-based thermoelectric hydrogel can generate a stable and continuous current (≈75 µA) under a

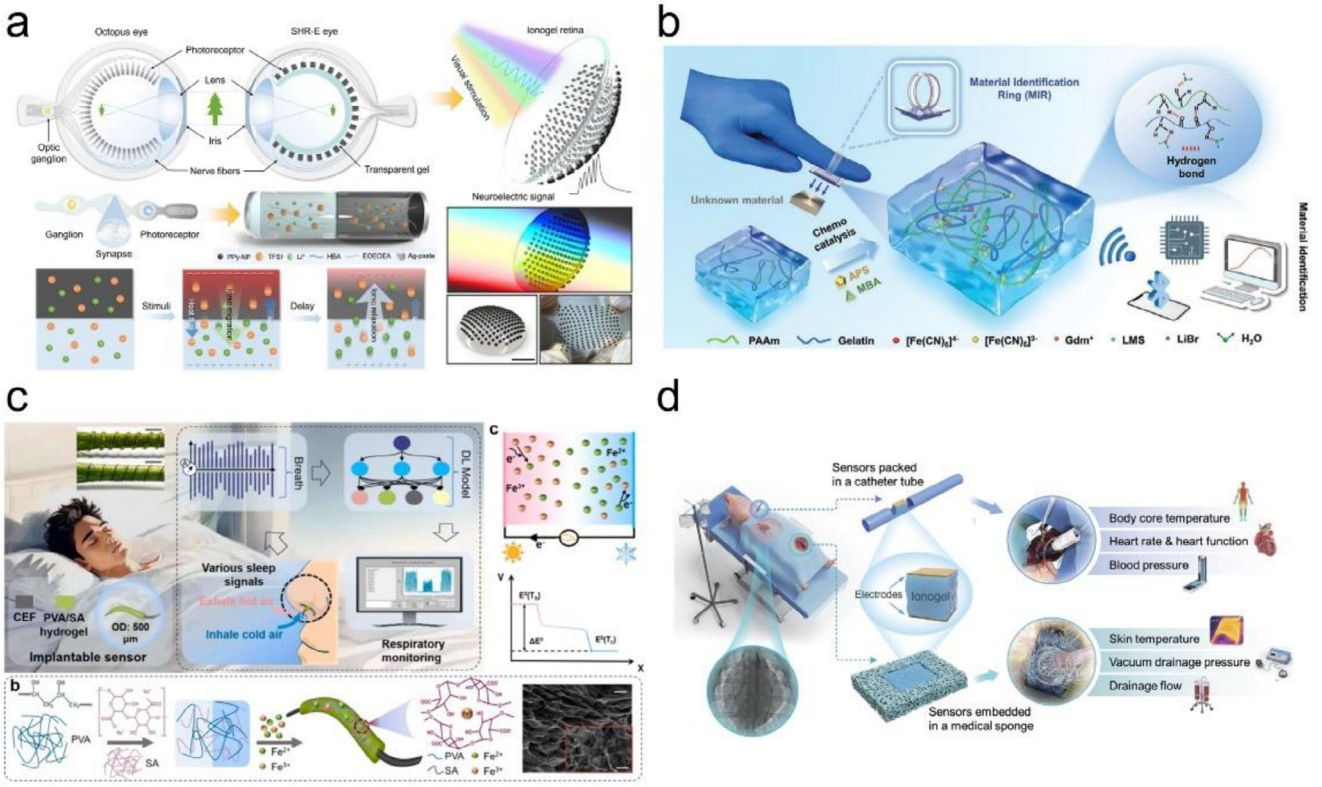

Figure 15. i-TE gels for human-machine interfaces. a) A self-driven retinomorphic eye with ionogel heterojunctions for broadband photoperception and a wide field of view. Reproduced under the terms of the CC-BY 4.0 license.[10] Copyright 2024, The Authors, Springer Nature. b) Self-powered, machine-learning material identification ring made from double-network i-TE gels. Reproduced with permission.[119] Copyright 2024, Wiley-VCH. c) Deep-learning-assisted i-TE gel-based fiber sensor for in-nostril respiratory monitoring. Reproduced with permission.[125] Copyright 2025, Elsevier. d) Self-powered multimodal medical sensors made from piezoelectric-augmented i-TE gels. Reproduced with permission.[126] Copyright 2024, Wiley-VCH.

temperature difference of 40 K. By converting the temperature differential between the interior and exterior of windows into electricity, smart windows can significantly enhance the energy conversion efficiency of modern buildings.

The i-TE gels can generate electricity by harnessing heat from flames, and they can also respond to rapid temperature increases, thereby triggering fire-warning systems. Jiang et al. prepared an i-TE gel with flame-retardant functionality through free-radical polymerization (Figure 14c).[115] The i-TE gel exhibits excellent flame retardancy, self-adhesive properties, and high thermopower (3.04 mV K^{-1}). When exposed to flames, this i-TE gel can activate a fire alarm and generate a voltage exceeding 100 mV. Zhao et al. fabricated a phosphorous-containing ionic liquid (PIL)-based ionogels (PILGs) that demonstrate excellent ionic conductivity (1.33 S m^{-1}) and high thermopower (1.31 mV K^{-1}) (Figure 14d).[116] The PILGs can provide flame retardancy and sensitive fire-warning capabilities to combustible materials. Additionally, PILGs exhibit high durability in extreme environments because due to the excellent thermal stability and low volatility of the PIL. These PILGs can be utilized as thermoelectric capacitors to power fire-warning circuit and electronics devices.

7.3. i-TE Gels-based Devices for Multimodal Physiological Signal Monitoring

Thermoelectric devices present promising applications in human-machine interfaces. Luo et al. have developed an artificial, self-powered, hemispherical retinomorphic eye (SHR-E), which features an ionogel heterojunction forest that functions as a photoreceptor (**Figure 15a**).[10] Drawing inspiration from the octopus's eye, they embed an array of photosensitive heterojunctions onto the surface of a transparent ionogel hemisphere, creating a retina-like pillar forest. This SHR-E device functions effectively as an optical-to-electrical converter while also exhibits neuroelectric plasticity. Unlike previous self-powered optical synapses that relied on the photovoltaic effect, the self-powering capability of SHR-E is primarily driven by selective ion diffusion within the ionogel, induced by the photothermoelectric effect. Furthermore, the SHR-E's exceptional conformal and stretchable properties allow the artificial retina to adhere seamlessly to surfaces with complex geometries, thereby enhancing its potential for diverse applications.

Tian et al. developed a self-healing thermoelectric hydrogel composed of poly(vinyl alcohol) and low acyl gellan gum,

utilizing $[Fe(CN)_6]^{4-/3-}$ as the redox couple.[117] A passive conformal wristband based on the i-TE hydrogel was created for the monitoring of multiple physiological signals, including body temperature, pulse rate, and sweat content, without the need for decoupling. Thermoelectric hydrogels that integrate temperature and strain sensing capabilities are in high demand for human-machine interfaces and wearable devices. Wu et al reported an i-TE hydrogel exhibiting high toughness and temperature responsiveness through the Hofmeister effect.[118] This i-TE hydrogel, functioning as a dual-responsive sensor, was integrated into a robotic hand and combined with feedback mechanisms based on deep learning. This device can issue temperature warnings at various levels, achieving a recognition accuracy of 95.3%.

Zhang et al. have made significant contributions to the field of self-powered sensing applications of i-TE gels, including identity recognition,[119,120]grip posture assessment,[121] sign language and object recognition,[122] multi-point fatigue monitoring,[123] and mental monitoring.[124] Touch is one of the most important ways for humans to explore the world. Zhang et al. designed a self-powered material identification ring (MIR) based on a thermoelectric double-network hydrogel that triggers a thermoelectric response to temperature changes (Figure 15b).[119] By analyzing the voltage signals associated with interfacial heat transfer generated upon contact with various materials, they successfully identified seven materials with an accuracy of up to 97.2%. Continuous monitoring of breathing patterns is vital for diagnosing diseases. Guo et al. created a self-powered intranasal hydrogel sensor for interference-resistant respiratory monitoring, using a dual-network i-TE gel (Figure 15c).[125] This innovative sensor generates thermoelectric signals in the nasal cavity by leveraging the temperature difference between exhaled air and skin, minimizing external interference. With deep learning, the system can identify seven distinct breathing patterns, achieving an accuracy of 97.1% and providing timely alerts for high-risk respiratory symptoms.

Pai et al. designed an i-TE gel based multimodal sensor that combines the i-TE effect of ionic liquids and the piezoelectric effect of a PVDF polymer networks (Figure 15d).[126] When the temperature gradient and pressure field are aligned, both factors generate voltage, while the piezoelectric effect amplifies the separation of cations and anions. This leads to a synergistic enhancement of i-TE potential. Additionally, the presence of water in the gel enhances ionic transport, thereby increasing the thermoelectric potential. An ionic gel sensor integrated into an arterial catheter, designed to leverage the material's dual sensitivity to temperature and pressure. Experiments conducted using a hemorrhagic shock model with pigs demonstrated the sensor's capability to accurately detect vital signs, including blood pressure, heart rate, surface temperature, core body temperature, and blood loss. This highlights the sensor's potential applications in medical monitoring.

7.4. i-TE Gels for Biomedical Applications

The endogenous electric field (EEF) is vital for wound healing, but electrolyte loss can weaken it.[127–129] Conventional direct current can cause thermal damage to wounds, whereas alternating current fails to mimic the direction of the EEF at the wound site. Emerging power supply methods, such as triboelectric and piezoelectric systems, require external triggers and often produce unstable voltage outputs. Therefore, designing dressings that restore the EEF and possess antibacterial properties is essential for effective wound healing. Yan et al. created a wearable thermoelectric dressing from polycationic hydrogels that generates thermoelectric potential by utilizing the temperature difference between the infected wound and the environment (**Figure 16a**).[130] This i-TE dressing reshapes the EEF and promotes healing through anti-inflammatory and antibacterial effects. The dressing accelerates wound healing by promoting cell proliferation, migration, angiogenesis, and collagen deposition, providing an effective solution for wound care.

Diabetic ulcers are a major cause of amputations and fatalities among diabetic patients. Severe electrolyte loss in these ulcers can result in a deficiency of endogenous electric fields, while disordered glucose metabolism and oxidative stress may cause endothelial dysfunction. Peng et al. developed a wireless smart thermoelectric hydrogel drug dressing containing a vascular-targeting exosome from ginseng (Figure 16b).[17] This dressing generates a biomimetic electric field and releases angiogenic signals to enhance healing and vascular reconstruction in challenging diabetic ulcers. This i-TE gel has been shown to promote re-epithelialization, dermal regeneration, and neovascular network reconstruction in diabetic mouse models. Additionally, single-cell RNA sequencing has revealed how i-TE gel regulates fibroblasts, endothelial cells, and inflammatory cells in the repair of diabetic ulcers. This study introduces a novel method for generating wireless passive electric fields through a light-heat-electric cascade effect, offering innovative concepts and support for thermoelectric materials in biomedicine and smart wearable medical devices.

Photothermal therapy (PTT) has garnered increasing attention due to its high accuracy and selectivity in tumor ablation and cancer treatment.[131] However, imprecise thermal regulation can damage adjacent healthy tissues, potentially leading to tumor invasion and recurrence. Xu et al. developed an innovative photothermoelectric (PTE) cobalt-infused chitosan hydrogel for precise temperature-regulated PTT, which features exceptional biocompatibility and desirable mechanical properties. The PTE responses demonstrate a linear correlation between temperature variations and resistance changes, enabling accurate control of PTT temperature through the monitoring of electrical signals. This thermoelectric hydrogel can function as a self-feedback platform to enhance the efficiency of photothermal therapy.

8. Challenges and Perspectives

Though thermoelectric hydrogels exhibit significant potential in energy harvesting and thermal sensing, they still face challenges such as improving efficiency, stability, and achieving system integration. Future research should explore new materials and structural designs to promote the application of these i-TE gels in various fields, including energy harvesting and wearable devices (**Figure 17**).

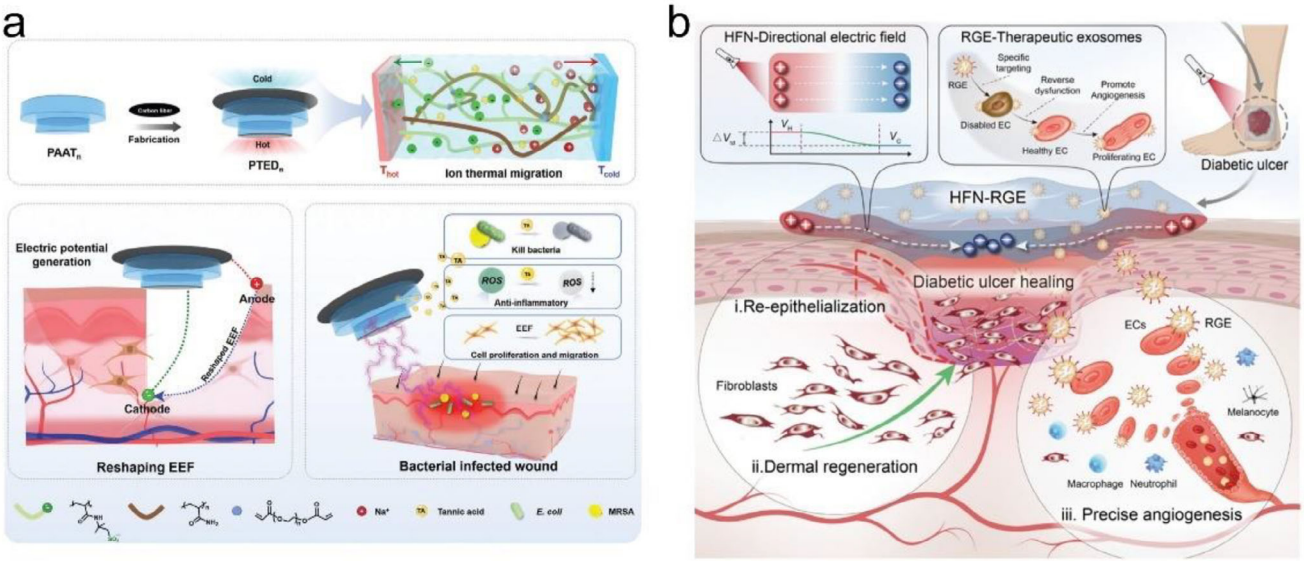

Figure 16. i-TE gels for biomedical applications. a) An i-TE gel dressing that reshapes the endogenous electric field by using the temperature difference between infected wounds and the environment. Reproduced with permission.[130] Copyright 2024, Wiley-VCH. b) Wireless i-TE hydrogel accelerates diabetic ulcer repair by mimicking electric fields and angiogenic signals. Reproduced with permission.[17] Copyright 2025, Wiley-VCH.

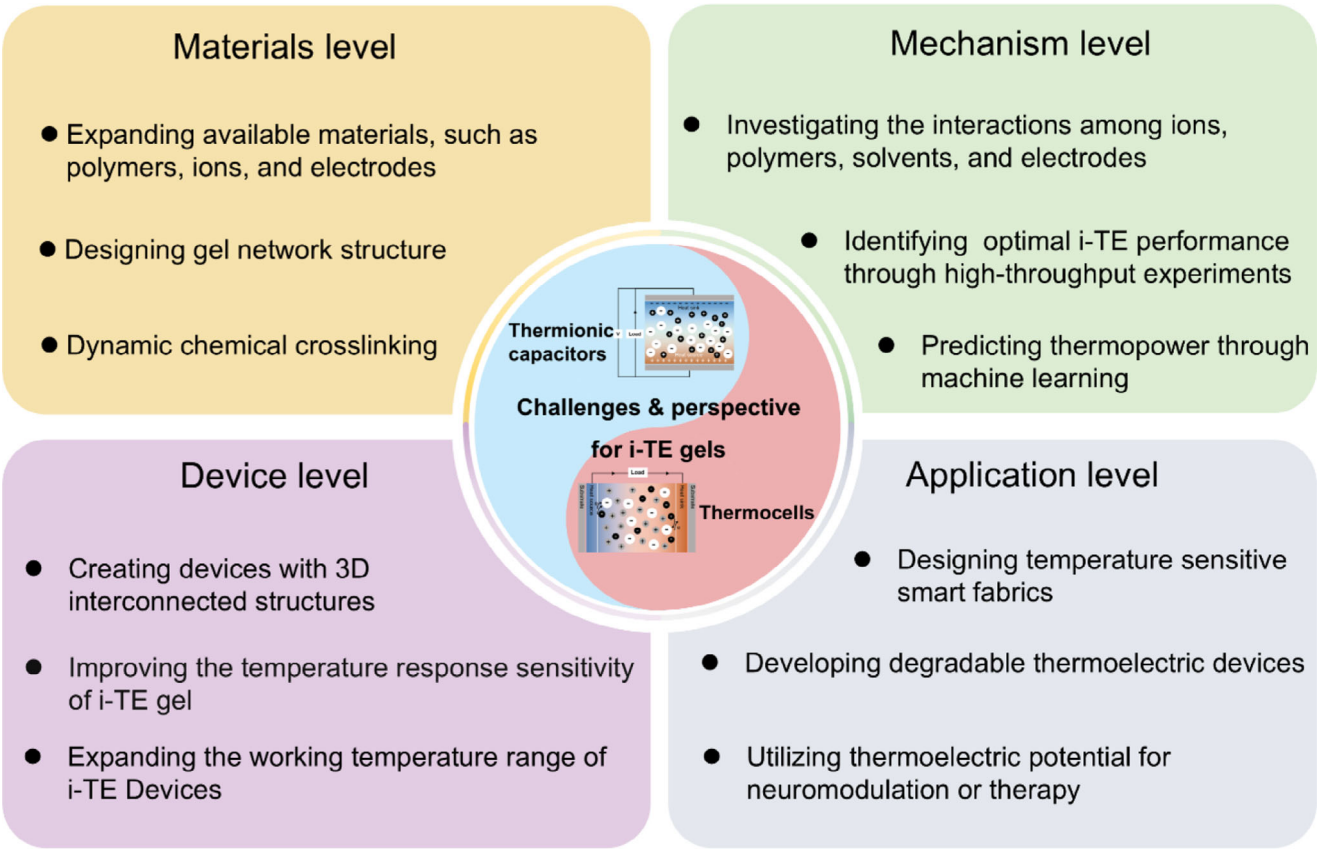

Figure 17. Challenges and perspectives of i-TE gels and devices.

8.1. Enhancing the Mechanical Performance of i-TE Gels

Various strategies have been employed to address this issue, including the use of multiple-hydrogen bond reinforced polyurethane as a polymer matrix and the implementation of double network structures. The trade-off between high i-TE performance and the mechanical durability of i-TE gels can be alleviated by optimizing the network structure. The toughness of i-TE gels can be improved by incorporating sacrificial bonds into the polymer network, such as hydrogen bonds, double networks and crystallization. Fatigue resistance in i-TE gels can be achieved through bionic mechanical training for hierarchical fibrils and aligned nanochannels, or by developing a dense network structure with enhanced entanglements between polymer chains. These distinctive properties position i-TE gels as promising energy solutions for flexible and wearable electronics.

It is essential to equip the i-TE gels with self-healing capabilities, particularly at the device level. This feature enables devices to recover form mechanical damage while ensuring continuous and stable energy output. The self-healing ability facilitates the rapid assembly of the thermoelectric modules by connecting different p/n legs of the i-TE gels through a cutting and healing process. Additionally, the output voltage can be successfully adjusted to the desired value. Furthermore, by integrating self-healing electrolytes and electrodes, fully self-healable i-TE devices can be developed, leading to the creation of reconfigurable and wearable energy devices. These self-healable i-TE devices could significantly impact prosthetics and robotics by extending their service life while minimizing the risk of damage.

8.2. Modulating the Thermopower of i-TE Gels

By adjusting the ion-polymer interactions within i-TE gels, the thermal diffusion of anions and cations in the electrolyte can be effectively controlled, thereby modulating the thermopower. The i-TE gels consist of solid networks and liquid electrolytes. The structure of these solid networks is essential for the mechanical and electrical properties of the i-TE gels. By modulating the interactions between solvent and polymer in i-TE gels, both mechanical and electrical properties can be improved. Acetone is an effective solvent for poly(vinylidene fluoride-*co*-hexafluoropropylene) (PVDF-HFP), whereas ethanol is regarded as a poor solvent. Thermopower and conductivity are significantly enhanced by engineering the polymer networks with antisolvents. In the typical capacitive operating mode of thermionic capacitors, ions migrate across the i-TE gels from the hot side to the cold side, accumulating at the electrode interface. During the charging and discharging cycles, it is essential to repeatedly establish and remove the heat source to facilitate the back-and-forth movement of ions, which presents practical challenges.

A comprehensive understanding of intermolecular interactions, along with a summary of established principles for enhancing the performance of i-TE gels can provide valuable insights for the design of high-performance i-TE gels. The integration of computational simulations with artificial intelligence and big data technologies shows promise in predicting the performance of i-TE gels, including their flexibility, stretchability, self-healing properties, thermopower, and ionic figure of merit.[132] This approach enables the design of i-TE gels with customized properties to meet the requirements of various application scenarios.

8.3. Expanding the Application Area of i-TE Gels

Owing to their exceptional flexibility, stretchability and durability, the application areas of ionic gels can be expanded to include wearable technology, implantable self-powered medical devices, and outdoor applications. Wearable, maintenance-free power sources have attracted considerable research interest due to the rise of the Internet of Things (IoT). Various methods have been explored to harvest energy from human activities, including walking, breathing, and blood circulation. Among these techniques, i-TE generators, such as thermionic capacitors or thermocells, can effectively harvest energy from the human body, providing a consistent and uninterrupted power source for wearable electronic devices. Additionally, ionic gels can accurately detect temperature changes due to their high thermopower. By balancing thermoelectric performance with biocompatibility, ionic gels can be utilized in vivo for self-powered medical devices. These gels are capable of harvesting thermal energy and converting it into electricity. They can capture dissipated body heat generated from muscle activity, blood circulation, and metabolic reactions to power implantable medical devices. In addition to energy harvesting, i-TE gels can function as self-powered sensors to monitor body temperature or the temperature fluctuations of the skin and organs, thereby reflecting the physiological state of the body. Furthermore, i-TE gels can also serve as electrical stimulators to activate organs such as the spinal cord, heart, and brain, offering treatment for chronic pain, irregular heart rates, and Parkinson's disease.

In summary, i-TE gels have emerged as a prominent area of research in materials science and engineering due to their unique properties and extensive application potential. As research progresses, these gels are expected to play a crucial role in energy conversion and human-computer interfaces.

9. Conclusions

I-TE gels, emerging as a prominent category of thermoelectric materials, have garnered attention due to their high thermopower, stretchability, adaptability, and potential for large-scale fabrication. This review summarizes the state-of-the-art advancements in the field of i-TE gels and presents their potential applications. The difference in thermodiffusion rates between cations and anions within the polymer matrix determines both the sign and magnitude of thermopower. The substantial thermopower of ionic gels enables the conversion of low-grade heat into electricity and demonstrates an ultra-sensitive response to temperature fluctuations. With their exceptional stretchability and adaptability, i-TE gels can be utilized in physiological monitoring, human-machine interfaces, and various biomedical applications. A comprehensive understanding of the interactions among polymers, ions, solvents, and electrodes is essential for enhancing the thermoelectric performance of ionic gels. The journey of i-TE gels has only just begun. Future research should concentrate on elucidating the mechanisms for designing high-performance i-TE gels while also expanding their application areas.

Acknowledgements

This work was supported by the National Natural Science Foundation of China (52403212, T2125003, 52472174), the Natural Science Foundation of Beijing Municipality (25JL006), and the Fundamental Research Funds for the Central Universities.

Conflict of Interest

The authors declare no conflict of interest.

Author Contributions

M.X. and J.M. wrote the manuscript. H.Z. provided suggestions on the Figures. Z.W. and Z.L. supervised the overall literature research. All the authors are involved in the discussion of the final manuscript.

Keywords

human-machine interfaces, ionic gels, low-grade heat harvesting, thermal sensing, thermoelectrics

Received: April 4, 2025
Revised: June 23, 2025
Published online:

[1] X. Shi, J. He, *Science* **2021**, *371*, 343.
[2] B. Russ, A. Glaudell, J. J. Urban, M. L. Chabinyc, R. A. Segalman, *Nat. Rev. Mater.* **2016**, *1*, 16050.
[3] J. Duan, B. Yu, K. Liu, J. Li, P. Yang, W. Xie, G. Xue, R. Liu, H. Wang, J. Zhou, *Nano Energy* **2019**, *57*, 473.
[4] T. Li, X. Zhang, S. D. Lacey, R. Mi, X. Zhao, F. Jiang, J. Song, Z. Liu, G. Chen, J. Dai, Y. Yao, S. Das, R. Yang, R. M. Briber, L. Hu, *Nat. Mater.* **2019**, *18*, 608.
[5] D. Zhao, A. Martinelli, A. Willfahrt, T. Fischer, D. Bernin, Z. U. Khan, M. Shahi, J. Brill, M. P. Jonsson, S. Fabiano, X. Crispin, *Nat. Commun.* **2019**, *10*, 1093.
[6] C.-G. Han, X. Qian, Q. Li, B. Deng, Y. Zhu, Z. Han, W. Zhang, W. Wang, S.-P. Feng, G. Chen, W. Liu, *Science* **2020**, *368*, 1091.
[7] S. Li, Q. Zhang, *Joule* **2020**, *4*, 1628.
[8] B. Chen, Q. Chen, S. Xiao, J. Feng, X. Zhang, T. Wang, *Sci. Adv.* **2021**, *7*, abi7233.
[9] Y. Li, Q. Li, X. Zhang, B. Deng, C. Han, W. Liu, *Adv. Energy Mater.* **2022**, *12*, 2103666.
[10] X. Luo, C. Chen, Z. He, M. Wang, K. Pan, X. Dong, Z. Li, B. Liu, Z. Zhang, Y. Wu, C. Ban, R. Chen, D. Zhang, K. Wang, Q. Wang, J. Li, G. Lu, J. Liu, Z. Liu, W. Huang, *Nat. Commun.* **2024**, *15*, 3086.
[11] M. Yang, Y. Hu, X. Wang, H. Chen, J. Yu, W. Li, R. Li, F. Yan, *Adv. Mater.* **2024**, *36*, 2312249.
[12] D. Zhao, H. Wang, Z. U. Khan, J. C. Chen, R. Gabrielsson, M. P. Jonsson, M. Berggren, X. Crispin, *Energy Environ. Sci.* **2016**, *9*, 1450.
[13] P. Yang, K. Liu, Q. Chen, X. Mo, Y. Zhou, S. Li, G. Feng, J. Zhou, *Angew. Chem., Int. Ed.* **2016**, *55*, 12050.
[14] M. Xiao, Y. Yao, W. Liu, *Sci. China Technol. Sci.* **2022**, *66*, 267.
[15] J. Sun, Y. Liu, J. Wei, P. Wei, T. Chen, *Chem. Eng. J.* **2024**, *485*, 149836.
[16] Y. Han, H. Wei, Y. Du, Z. Li, S. P. Feng, B. Huang, D. Xu, *Adv. Sci.* **2023**, *10*, 2302685.
[17] M. Tan, Y. Liu, Y. Wang, Y. Li, C. Wu, Z. Jiang, L. Peng, *Adv. Funct. Mater.* **2025**, 2425610.
[18] L. Liu, D. Zhang, P. Bai, Y. Mao, Q. Li, J. Guo, Y. Fang, R. Ma, *Adv. Mater.* **2023**, *35*, 2300696.
[19] D.-H. Kim, Z. A. Akbar, Y. T. Malik, J.-W. Jeon, S.-Y. Jang, *Nat. Commun.* **2023**, *14*, 3246.
[20] W. Zhou, L. Zhao, H. Cheng, J. Chen, J. Ouyang, *Chem. Eng. J.* **2023**, *477*, 147257.
[21] S. Sun, X. L. Shi, W. Lyu, M. Hong, W. Chen, M. Li, T. Cao, B. Hu, Q. Liu, Z. G. Chen, *Adv. Funct. Mater.* **2024**, *34*, 2402823.
[22] C. Chi, G. Liu, M. An, Y. Zhang, D. Song, X. Qi, C. Zhao, Z. Wang, Y. Du, Z. Lin, Y. Lu, H. Huang, Y. Li, C. Lin, W. Ma, B. Huang, X. Du, X. Zhang, *Nat. Commun.* **2023**, *14*, 306.
[23] K. Jiang, J. Jia, Y. Chen, L. Li, C. Wu, P. Zhao, D. Y. Zhu, W. Zeng, *Adv. Energy Mater.* **2023**, *13*, 2204357.
[24] Y. Li, S. Wang, M. Yu, H. Li, B. Li, K. Zhu, W. Liu, *Adv. Energy Mater.* **2024**, *15*, 2402621.
[25] J. Duan, B. Yu, L. Huang, B. Hu, M. Xu, G. Feng, J. Zhou, *Joule* **2021**, *5*, 768.
[26] Y. Wang, L. Yang, X. L. Shi, X. Shi, L. Chen, M. S. Dargusch, J. Zou, Z. G. Chen, *Adv. Mater.* **2019**, *31*, 1807916.
[27] Y. Jia, Q. Jiang, H. Sun, P. Liu, D. Hu, Y. Pei, W. Liu, X. Crispin, S. Fabiano, Y. Ma, Y. Cao, *Adv. Mater.* **2021**, *33*, 2102990.
[28] Z. Dong, Q. Xiang, Z. Zhang, J. Tang, F. Li, K. Sun, S. Chen, *CCS Chem* **2024**, *6*, 2627.
[29] D. Zhao, A. Würger, X. Crispin, *J. Energy Chem.* **2021**, *61*, 88.
[30] A. Würger, *Phys. Rev. Res.* **2020**, *2*, 042030.
[31] M. Yu, H. Li, Y. Li, S. Wang, Q. Li, Y. Wang, B. Li, K. Zhu, W. Liu, *EnergyChem* **2024**, *6*, 100123.
[32] Z. Li, Y. Xu, X. Zhang, *EnergyChem* **2024**, *6*, 100136.
[33] X. Sun, A. Lu, *J. Polym Sci.* **2023**, *62*, 266.
[34] H. Cheng, X. He, Z. Fan, J. Ouyang, *Adv. Energy Mater.* **2019**, *9*, 1901085.
[35] Z. Liu, H. Cheng, Q. Le, R. Chen, J. Li, J. Ouyang, *Adv. Energy Mater.* **2022**, *12*, 2200858.
[36] Z. Liu, H. Cheng, H. He, J. Li, J. Ouyang, *Adv. Funct. Mater.* **2021**, *32*, 2109772.
[37] Z. A. Akbar, Y. T. Malik, D. H. Kim, S. Cho, S. Y. Jang, J. W. Jeon, *Small* **2022**, *18*, 2106937.
[38] M. Li, H. Xu, M. Luo, X. Qing, W. Wang, W. Zhong, Q. Liu, Y. Wang, L. Yang, X. Zhu, D. Wang, *Chem. Eng. J.* **2024**, *485*, 149784.
[39] Y. Fang, H. Cheng, H. He, S. Wang, J. Li, S. Yue, L. Zhang, Z. Du, J. Ouyang, *Adv. Funct. Mater.* **2020**, *30*, 2004699.
[40] J. Xu, H. Wang, X. Du, X. Cheng, Z. Du, H. Wang, *ACS Appl. Mater. Interfaces* **2021**, *13*, 20427.
[41] Y. Zhao, H. Cheng, Y. Li, J. Rao, S. Yue, Q. Le, Q. Qian, Z. Liu, J. Ouyang, *J. Mater. Chem. A* **2022**, *10*, 4222.
[42] W. Zhao, Y. Zheng, M. Jiang, T. Sun, A. Huang, L. Wang, W. Jiang, Q. Zhang, *Sci. Adv.* **2023**, *9*, adk2098.
[43] C. Xu, Y. Sun, J. Zhang, W. Xu, H. Tian, *Adv. Energy Mater.* **2022**, *12*, 2201542.
[44] C. Tian, C. Bai, T. Wang, Z. Yan, Z. Zhang, K. Zhuo, H. Zhang, *Nano Energy* **2023**, *106*, 108077.
[45] Z. Lei, W. Gao, W. Zhu, P. Wu, *Adv. Funct. Mater.* **2022**, *32*, 2201021.
[46] Y. Ye, H. Oguzlu, J. Zhu, P. Zhu, P. Yang, Y. Zhu, Z. Wan, O. J. Rojas, F. Jiang, *Adv. Funct. Mater.* **2022**, *33*, 2209787.
[47] T. H. Park, B. Kim, S. Yu, Y. Park, J. W. Oh, T. Kim, N. Kim, Y. Kim, D. Zhao, Z. Ullah Khan, S. Lienemann, X. Crispin, K. Tybrandt, C. Park, S. C. Jun, *Nano Energy* **2023**, *114*, 108643.
[48] D. Zhang, Y. Mao, F. Ye, Q. Li, P. Bai, W. He, R. Ma, *Energy Environ. Sci.* **2022**, *15*, 2974.
[49] M. Zhang, Q. Fu, H. Deng, *Chem. Eng. J.* **2024**, *486*, 150307.
[50] C. Y. Lee, S. H. Hong, C. L. Liu, *Macromol. Rapid Commun.* **2025**, *46*, 2400837.
[51] Q. Le, H. Cheng, J. Ouyang, *Chem. Eng. J.* **2023**, *469*, 143828.

[52] S.-H. Hong, C.-C. Hsu, T.-H. Liu, T.-C. Lee, S.-H. Tung, H.-L. Chen, J. Yu, C.-L. Liu, *Mater. Today Energy* **2024**, *42*, 101546.
[53] Y. Hu, D. Xie, Z. Liu, B. Xie, M. Li, G. Chen, Z. Liu, *J. Mater. Chem. A* **2024**, *12*, 17315.
[54] Z. Xu, S. Lin, Y. Yin, X. Gu, *Chem. Eng. J.* **2024**, *493*, 152734.
[55] X. Sun, M. Zhang, H. Qi, P. Chen, J. Zhang, A. Lu, *Adv. Funct. Mater.* **2024**, *35*, 2419762.
[56] J. Hu, J. Wei, J. Li, L. Bai, Y. Liu, Z. Li, *Energy Environ. Sci.* **2024**, *17*, 1664.
[57] J. Shen, Y. Ma, C. Yang, S. Liu, J. Li, Z. Chen, B. Tian, S. Li, *J. Mater. Chem. A* **2022**, *10*, 7785.
[58] Y. Liu, J. Zhou, Y. Li, X. Sun, Z. Wang, H. Yang, C. Wang, *Adv. Funct. Mater.* **2024**, *34*, 2400203.
[59] J. Yu, M. Luo, X. Zhu, X. Qing, W. Wang, W. Zhong, Q. Liu, Y. Wang, Y. Lu, M. Li, D. Wang, *Chem. Eng. J.* **2024**, *488*, 150638.
[60] Y. Chen, G. Hong, L. Li, Q. Qu, G. Li, J. Wu, L. Ge, *Chem. Eng. J.* **2024**, *483*, 149344.
[61] N. Menéndez, M. Muddasar, M. A. Nasiri, A. Cantarero, C. M. Gómez, R. Muñoz-Espí, M. N. Collins, M. Culebras, *ACS Appl. Polym. Mater.* **2025**, *7*, 3093.
[62] K. Liu, J. Lv, G. Fan, B. Wang, Z. Mao, X. Sui, X. Feng, *Adv. Funct. Mater.* **2021**, *32*, 2107105.
[63] Z. Wu, B. Wang, J. Li, R. Wu, M. Jin, H. Zhao, S. Chen, H. Wang, *Nano Lett.* **2022**, *22*, 8152.
[64] Y. Zong, H. Li, X. Li, J. Lou, Q. Ding, Z. Liu, Y. Jiang, W. Han, *Chem. Eng. J.* **2022**, *433*, 134550.
[65] J. Li, S. Chen, Z. Wu, Z. Han, X. Qu, M. Jin, Y. Jia, Z. Zhou, H. Wang, *Nano Energy* **2023**, *112*, 108482.
[66] Z. Wu, B. Wang, J. Li, Y. Jia, S. Chen, H. Wang, L. Chen, L. Shuai, *Nano Lett.* **2023**, *23*, 10297.
[67] Q. Chen, B. Chen, S. Xiao, J. Feng, J. Yang, Q. Yue, X. Zhang, T. Wang, *ACS Appl. Mater. Interfaces* **2022**, *14*, 19304.
[68] Y. He, Q. Zhang, H. Cheng, Y. Liu, Y. Shu, Y. Geng, Y. Zheng, B. Qin, Y. Zhou, S. Chen, J. Li, M. Li, G. O. Odunmbaku, C. Li, T. Shumilova, J. Ouyang, K. Sun, *J. Phys. Chem. Lett.* **2022**, *13*, 4621.
[69] Z. A. Akbar, J.-W. Jeon, S.-Y. Jang, *Energy Environ. Sci.* **2020**, *13*, 2915.
[70] Y. T. Malik, Z. A. Akbar, J. Y. Seo, S. Cho, S. Y. Jang, J. W. Jeon, *Adv. Energy Mater.* **2021**, *12*, 2103070.
[71] Z. Zhao, Y.-P. Hu, K.-Y. Liu, W. Yu, G.-X. Li, C.-Z. Meng, S.-J. Guo, *Gels* **2023**, *9*, 257.
[72] W. Gao, Z. Lei, C. Zhang, X. Liu, Y. Chen, *Adv. Funct. Mater.* **2021**, *31*, 2104071.
[73] Z. Lei, W. Gao, P. Wu, *Joule* **2021**, *5*, 2211.
[74] Y.-T. Lin, C.-C. Hsu, S.-H. Hong, L.-C. Lee, U. S. Jeng, H.-L. Chen, S.-H. Tung, C.-L. Liu, *J. Power Sources* **2024**, *609*, 234647.
[75] P. Peng, J. Zhou, L. Liang, X. Huang, H. Lv, Z. Liu, G. Chen, *Nano Micro Lett.* **2022**, *14*, 81.
[76] D. Zhang, Y. Zhou, Y. Mao, Q. Li, L. Liu, P. Bai, R. Ma, *Nano Lett.* **2023**, *23*, 11272.
[77] X. Lyu, Z. Lin, C. Huang, X. Zhang, Y. Lu, Z.-Z. Luo, P. Zhou, Z. Zou, *Chem. Eng. J.* **2024**, *493*, 152887.
[78] Y. Zhao, X. Fu, B. Liu, J. Sun, Z. Zhuang, P. Yang, J. Zhong, K. Liu, *Sci. China Mater.* **2023**, *66*, 1934.
[79] D. H. Ho, Y. M. Kim, U. J. Kim, K. S. Yu, J. H. Kwon, H. C. Moon, J. H. Cho, *Adv. Energy Mater.* **2023**, *13*, 2301133.
[80] C. Cho, B. Kim, S. Park, E. Kim, *Energy Environ. Sci.* **2022**, *15*, 2049.
[81] M. Li, M. Hong, M. Dargusch, J. Zou, Z.-G. Chen, *Trends Chem.* **2021**, *3*, 561.
[82] X. He, H. Sun, Z. Li, X. Chen, Z. Wang, Y. Niu, J. Jiang, C. Wang, *J. Mater. Chem. A* **2022**, *10*, 20730.
[83] X. Qian, Z. Ma, Q. Huang, H. Jiang, R. Yang, *ACS Energy Lett.* **2024**, *9*, 679.
[84] J. Liu, W. Zeng, X. Tao, *Adv. Funct. Mater.* **2022**, *32*, 2208286.
[85] X. Cheng, Y. Hu, P. Chen, H. Qi, A. Lu, *Chem. Eng. J.* **2024**, *498*, 155161.
[86] Q. Li, D. Yu, S. Wang, X. Zhang, Y. Li, S. P. Feng, W. Liu, *Adv. Funct. Mater.* **2023**, *33*, 2305835.
[87] W. Zhao, T. Sun, Y. Zheng, Q. Zhang, A. Huang, L. Wang, W. Jiang, *Adv. Sci.* **2022**, *9*, 2201075.
[88] D. Zhang, Y. Fang, L. Liu, Y. Zhou, P. Bai, Q. Li, J. Guo, R. Ma, *Adv. Energy Mater.* **2023**, *14*, 2303358.
[89] Q. Li, C.-G. Han, S. Wang, C.-C. Ye, X. Zhang, X. Ma, T. Feng, Y. Li, W. Liu, *eScience* **2023**, *3*, 100169.
[90] Q. Le, Z. Chen, H. Cheng, J. Ouyang, *Adv. Energy Mater.* **2023**, *13*, 2302472.
[91] B. Chen, X. Zhang, J. Yang, J. Feng, T. Wang, *ACS Appl. Mater. Interfaces* **2023**, *15*, 24483.
[92] Q. Hu, H. Li, X. Chen, Y. Wang, H. Wu, S. Guo, K. Xu, *Adv. Funct. Mater.* **2024**, *34*, 2406968.
[93] S. Liu, Y. Yang, H. Huang, J. Zheng, G. Liu, T. H. To, B. Huang, *Sci. Adv.* **2022**, *8*, abj3019.
[94] S. Liu, Y. Yang, S. Chen, J. Zheng, D. G. Lee, D. Li, J. Yang, B. Huang, *Nano Energy* **2022**, *100*, 107542.
[95] B. Guo, Y. Hoshino, F. Gao, K. Hayashi, Y. Miura, N. Kimizuka, T. Yamada, *J. Am. Chem. Soc.* **2020**, *142*, 17318.
[96] W. Zhao, Y. Zheng, A. Huang, M. Jiang, L. Wang, Q. Zhang, W. Jiang, *Adv. Mater.* **2024**, *36*, 2402386.
[97] S. Kim, M. Ham, J. Lee, J. Kim, H. Lee, T. Park, *Adv. Funct. Mater.* **2023**, *33*, 2305499.
[98] L. C. Lee, K. T. Huang, Y. T. Lin, U. S. Jeng, C. H. Wang, S. H. Tung, C. J. Huang, C. L. Liu, *Small* **2024**, *20*, 2311811.
[99] L. Chen, X. Rong, Z. Liu, Q. Ding, X. Li, Y. Jiang, W. Han, J. Lou, *Chem. Eng. J.* **2024**, *481*, 148797.
[100] K.-Y. Liu, Y.-P. Hu, W. Yu, C.-Z. Meng, S.-J. Guo, G.-X. Li, *Mater. Lett.* **2024**, *372*, 137038.
[101] S. Li, Y. Xu, Z. Li, S. Zhang, H. Dou, X. Zhang, *J. Mater. Chem. A* **2025**, *13*, 3913.
[102] C. Chi, M. An, X. Qi, Y. Li, R. Zhang, G. Liu, C. Lin, H. Huang, H. Dang, B. Demir, Y. Wang, W. Ma, B. Huang, X. Zhang, *Nat. Commun.* **2022**, *13*, 221.
[103] G. Li, D. Dong, G. Hong, L. Yan, X. Zhang, W. Song, *Adv. Mater.* **2019**, *31*, 1901403.
[104] L. Yang, J. Chen, C.-G. Han, Y. Zhu, C. Xie, Z. Liu, H. Wang, Y. Bao, D. Han, L. Niu, *Energy Environ. Sci.* **2025**, *18*, 2559.
[105] Y. Zhu, C.-G. Han, J. Chen, L. Yang, Y. Ma, H. Guan, D. Han, L. Niu, *Energy Environ. Sci.* **2024**, *17*, 4104.
[106] Y. He, S. Li, R. Chen, X. Liu, G. O. Odunmbaku, W. Fang, X. Lin, Z. Ou, Q. Gou, J. Wang, N. A. N. Ouedraogo, J. Li, M. Li, C. Li, Y. Zheng, S. Chen, Y. Zhou, K. Sun, *Nano Micro Lett.* **2023**, *15*, 101.
[107] Z. Zhou, Y. Wan, J. Zi, G. Ye, T. Jin, X. Geng, W. Zhuang, P. Yang, *Mater. Today Sustainability* **2023**, *21*, 100293.
[108] Y. Wang, Y. Dai, L. Li, L. Yu, W. Zeng, *Angew. Chem., Int. Ed.* **2023**, *62*, 202307947.
[109] Y. Li, Q. Li, X. Zhang, J. Zhang, S. Wang, L. Lai, K. Zhu, W. Liu, *Energy Environ. Sci.* **2022**, *15*, 5379.
[110] C.-G. Han, Y.-B. Zhu, L. Yang, J. Chen, S. Liu, H. Wang, Y. Ma, D. Han, L. Niu, *Energy Environ. Sci.* **2024**, *17*, 1559.
[111] S. Pu, Y. Liao, K. Chen, J. Fu, S. Zhang, L. Ge, G. Conta, S. Bouzarif, T. Cheng, X. Hu, K. Liu, J. Chen, *Nano Lett.* **2020**, *20*, 3791.
[112] J. Shen, X. Huang, Y. Dai, X. Zhang, F. Xia, *Nat. Commun.* **2024**, *15*, 9305.
[113] W. Zhao, Z. Lei, P. Wu, *Adv. Sci.* **2023**, *10*, 2300253.
[114] G. Xie, Y. Li, C. Wu, M. Cao, H. Chen, Y. Xiong, Y. Xu, H. Xie, W. Yu, *Chem. Eng. J.* **2024**, *481*, 148531.
[115] C. Jiang, X. Lai, Z. Wu, H. Li, X. Zeng, Y. Zhao, Q. Zeng, J. Gao, Y. Zhu, *J. Mater. Chem. A* **2022**, *10*, 21368.

[116] Y. Zhao, Q. Zeng, C. Jiang, X. Lai, H. Li, Z. Wu, X. Zeng, *Nano Energy* **2023**, *116*, 108785.
[117] C. Tian, S. A. Khan, Z. Zhang, X. Cui, H. Zhang, *ACS Sens.* **2024**, *9*, 840.
[118] X. Wu, X. Yang, P. Wang, Z. Wang, X. Fan, W. Duan, Y. Yue, J. Xie, Y. Liu, *ACS Sens.* **2024**, *9*, 4216.
[119] Y. Li, W. Wang, X. Cui, N. Li, X. Ma, Z. Wang, Y. Nie, Z. Huang, H. Zhang, *Small* **2024**, *21*, 2405911.
[120] X. Ma, W. Wang, X. Cui, Y. Li, K. Yang, Z. Huang, H. Zhang, *Small* **2024**, *20*, 2402700.
[121] S. Sang, C. Bai, W. Wang, S. A. Khan, Z. Wang, X. Yang, Z. Zhang, H. Zhang, *Nano Energy* **2024**, *123*, 109366.
[122] H. Yang, N. Li, K. Yang, L. Sun, H. Zhang, Z. Zhang, X. Cui, *Chem. Eng. J.* **2024**, *488*, 150816.
[123] X. Zhang, N. Li, X. Cui, Y. Li, Z. Wang, K. Zhuo, H. Zhang, *J. Mater. Chem. C* **2024**, *12*, 12064.
[124] Y. Li, N. Li, X. Zhang, J. Zhang, L. Sun, Z. Huang, H. Zhang, *J. Mater. Chem. A* **2025**, *13*, 10531.
[125] Y. Zhang, H. Wang, S. Ahmed Khan, J. Li, C. Bai, H. Zhang, R. Guo, *J. Colloid Interface Sci.* **2025**, *678*, 143.
[126] Y. H. Pai, C. Xu, R. Zhu, X. Ding, S. Bai, Z. Liang, L. Chen, *Adv. Mater.* **2024**, *37*, 2414663.
[127] R. Luo, B. Shi, D. Luo, Z. Li, *Sci. Bull.* **2023**, *68*, 1740.
[128] R. Luo, Y. Fan, Y. Qi, Y. Bai, M. Xiao, Y. Lv, J. Liang, M. Tang, J. Zhang, Z. Li, D. Luo, *Adv. Mater.* **2025**, *37*, 2419149.
[129] Z. Li, H. Wei, *Micro* **2024**, *4*, 823.
[130] S. Gao, Y. Rao, X. Wang, Q. He, M. Yang, Y. Wang, Y. Zhou, J. Guo, F. Yan, *Adv. Funct. Mater.* **2024**, *35*, 2415085.
[131] X. Ji, Z. Tang, H. Liu, Y. Kang, L. Chen, J. Dong, W. Chen, N. Kong, W. Tao, T. Xie, *Adv. Mater.* **2022**, *35*, 2207391.
[132] Y. Wu, D. Song, M. An, C. Chi, C. Zhao, B. Yao, W. Ma, X. Zhang, *Natl. Sci. Rev.* **2025**, *12*, nwae411.